nature of GABA as an excitatory molecule early in life, followed by a functional switch to an inhibitory species later in development. Furthermore, quantitative ^{1}H-MRS appears to be a useful, noninvasive tool for detecting inborn errors of GABA metabolism in the CNS.

Abbreviations

GABA-T	Gamma aminobutyric acid transaminase
^{1}H-MRS	Proton magnetic resonance spectroscopy
CNS	Central nervous system
SSADH	Succinic semialdehyde dehydrogenase
GHB	4-hydroxybutyrate
EEG	Electroencephalogram
CSF	Cerebrospinal fluid
DWI	Diffusion-weighted image
Glx	Glutamine/glutamate complex

Introduction

Disorders of gamma aminobutyric acid (GABA) metabolism are rare and manifest prominent neurological sequelae; 4-aminobutyrate aminotransferase (γ-aminobutyrate: GABA transaminase, or GABA-T; OMIM 137150) deficiency is characterized by severe psychomotor retardation, hypotonia, hyperreflexia, seizures, high-pitched cry, and growth acceleration, associated with early infantile death in two siblings (one family) (Jaeken et al 1984; Jakobs et al 1993). Succinic semialdehyde dehydrogenase (SSADH) deficiency [or 4-hydroxybutyric (GHB) aciduria] is the most prevalent of the GABA degradation disorders and one in which pharmacologically active GHB, as well as GABA, accumulate in patient body fluids (Jakobs et al 1993; Pearl et al 2007). Homocarnosinosis (homocarnosine is the GABA:L-histidine

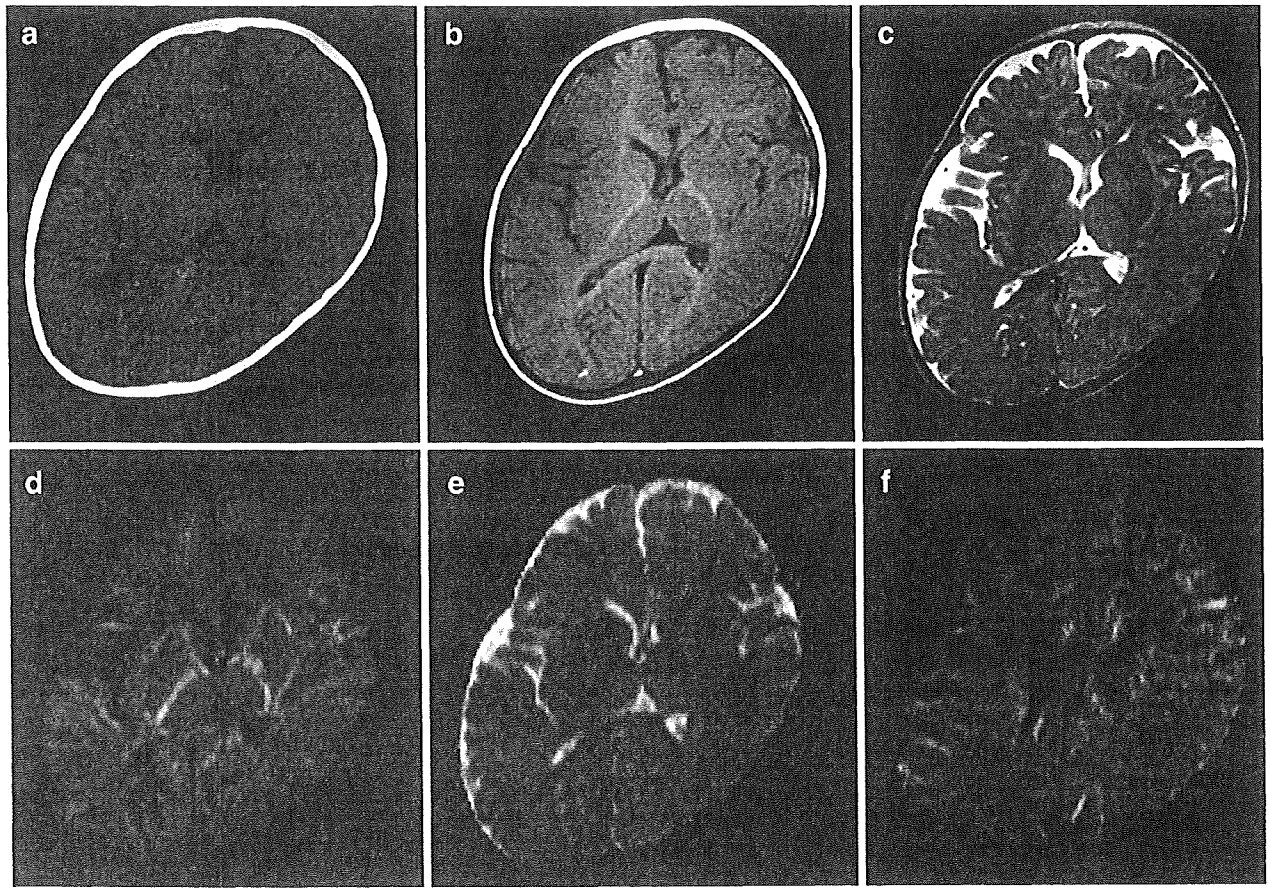

Fig. 1 Initial computed tomography (CT) and magnetic resonance imaging (MRI) findings at 8 months. Baseline CT (**a**), T1-weighted (**b**), T2-weighted (**c**), diffusion-weighted (**d**) axial MRI images, and apparent diffusion coefficients (ADC) map (**e**) at the level of the basal ganglia, and diffusion-weighted images (DWI) of the semioval center (**f**). CT (**a**) shows no particular abnormality, whereas T1-weighted (**b**) and T2-weighted (**c**) images suggest delayed myelination. Subcortical high white-matter signal on the T1-weighted image was not observed, and low signal on the T2-weighted image was limited to the posterior portion of the internal capsules and splenium of the corpus callosum. DWI (**d**, **f**) shows widespread high signals in the internal and external capsules and many parts of the subcortical white matter, with restricted diffusion (**e**)

conjugate) is very rare (two cases) and may represent an allelic form of carnosinase deficiency(Pearl et al 2007). Considering the inhibitory nature of GABA activity in the central nervous system (CNS), the paradoxical neurological phenomenon associated with seizures in cases of GABA excess is of interest. In this study, we detected elevated GABA in a patient by proton magnetic resonance spectroscopy (^{1}H-MRS) using the LCModel to quantify the spectra automatically. This method has potential application to neurological disorders such as GABA-T deficiency.

Case report

The patient was a Japanese female infant, born full term with normal delivery. She was the second child of healthy parents. There was no consanguinity or family history of neurological disorders. A 6-year-old sister was normal. Early infancy was unremarkable. At 7 months, she was evaluated for psychomotor retardation, hypotonia, bilateral intermittent esotropia, hyperreflexia, and positive Babinski reflex. There was no dysmorphy. At age 8 months, she was admitted with decreased consciousness 48 h after an acute febrile illness. Respiratory distress developed that required mechanical ventilation. Steroid pulse therapy was initiated for a suspected acute encephalopathy of unknown etiology. Segmental myoclonic jerks occurred and were difficult to control, but consciousness returned. Electroencephalography (EEG) revealed diffuse slow spike and wave discharges with 1- to 2-s periods of suppression. Phenobarbital, clonazepam, valproate, and midazolam could not completely control seizures. Limb motor conduction velocities were

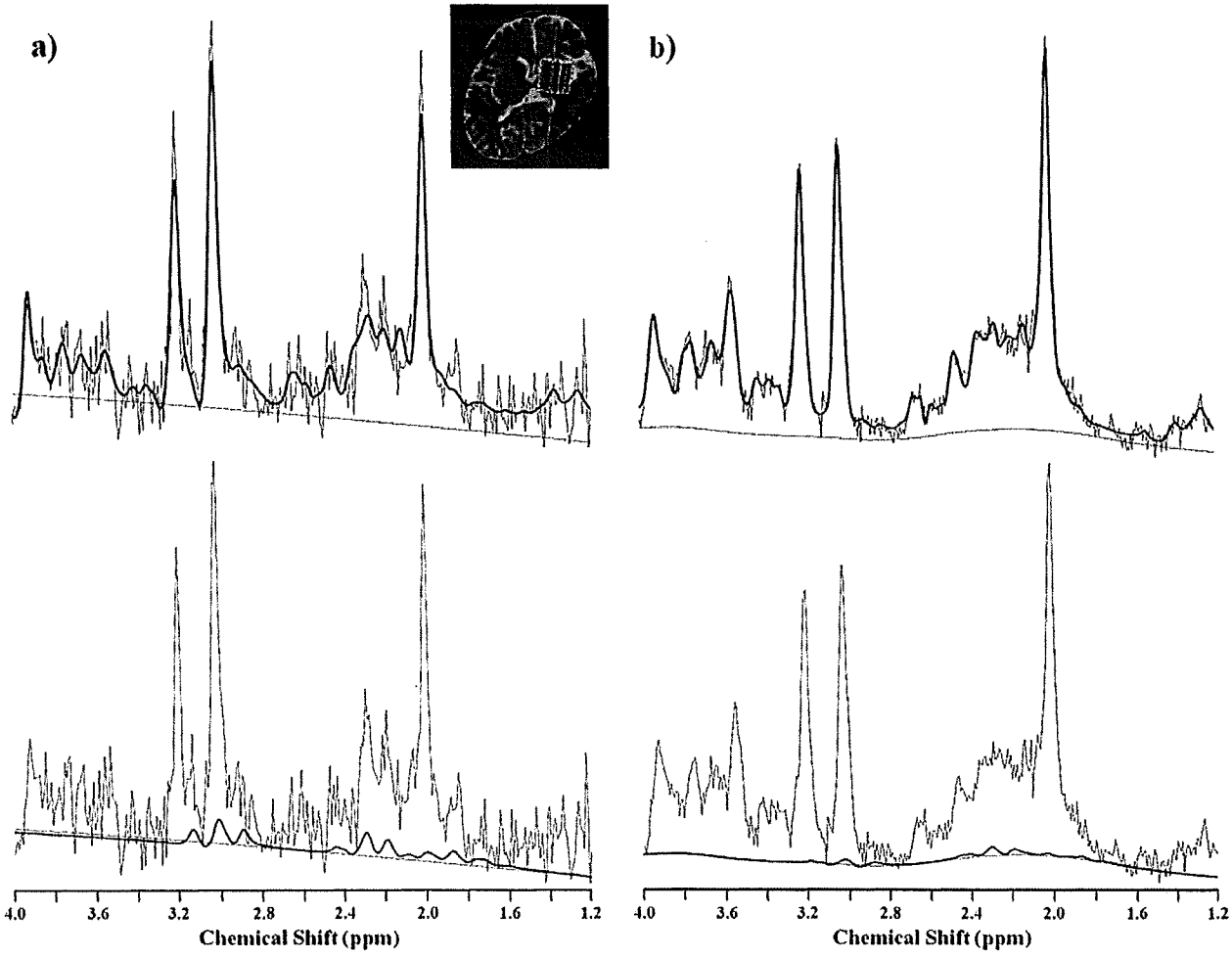

Fig. 2 LCModel outputs of in vivo proton magnetic resonance (MR) spectra from the basal ganglia (volume, 10–17.5 ml; TE/TR, 20–30/5000 ms; number of excitations 6). *Bold lines* indicate LCModel fitting, and *thin lines* indicate the original spectra. Patient with gamma aminobutyric acid transaminase (GABA-T) deficiency (8 months) (**a**), a control individual (7 months) (**b**). *Bold lines* in the *upper row* are the fitting curves of total spectra including all metabolites, and those in the *lower row* are fitting curves for GABA. The estimated absolute concentrations of GABA in patient and control are 2.9 and 0.8 mmol/l, respectively. Normal GABA spectrum exhibits a quintet ($^3CH_2$) at 1.89 ppm, a triplet ($^4CH_2$) at 2.28 ppm, and a multiplet resembling a triplet ($^2CH_2$) at 3.01 ppm(Govindaraju et al 2000)

within normal limits. Anthropomorphic parameters revealed accelerated height in late infancy [+2.5–3.0 standard deviation (SD)], with normal head circumference and decreased weight gain. At 8 months, her height was 76 cm (+3.0 SD), weight 6745 g (−1.7 SD), and head circumference 44 cm (−0.4 SD). Nasogastric tube feeding was started due to recurrent aspiration pneumonia. At 11 months, domiciliary oxygen was introduced because of chronic respiratory failure. At the age of 28 months, her height was 96 cm (+2.9 SD), weight 10.3 kg (−1.1 SD), and head circumference 46.5 cm (−0.7 SD). Febrile illness was consistently associated with neurological deterioration, and the patient progressed to opisthotonic posturing with generalized dystonia and segmental myoclonic jerks, which never resolved while awake.

Methods and results

Laboratory data

Routine laboratory tests were normal. Amino acid analysis showed elevated free GABA in the serum and cerebral spinal fluid (CSF) at 9 months of age (2.1 μmol/l and 1.26 μmol/l, respectively; normal range serum 0.12–0.50, CSF 0.04–0.12) (Jaeken et al 1984). Serum growth hormone was elevated (8.84 ng/ml; normal range 0.28–1.64). Insulin-like growth factor levels were relatively low (54 ng/ml; normal range 37–229). An absence of GHB in urine organic acid analysis precluded SSADH deficiency as a cause of increased GABA. β-alanine and homocarnosine were not detectable on the chromatogram, and their quantitative analyses were not performed.

Radiological findings

Bone age was 1 year 8 months at the age of 1 year 10 months (TW2 method). Initial brain computed tomography (CT) was unremarkable (Fig. 1a), and brain magnetic resonance imaging (MRI) (1.5 T) suggested mild delay in myelination (Fig. 1b, c) without structural anomalies. Diffusion weighted images (DWI) revealed high signal intensity in the internal and external capsules and much of the subcortical white matter, with restricted apparent diffusion coefficiency (Fig. 1d–f). For quantitative ^{1}H-MRS (age 8 months), locations were placed in the white matter (semioval center) and the basal ganglia (10 ml). ^{1}H-MR spectra were obtained using the stimulated-echo acquisition mode (STEAM) sequence (Frahm et al 1987) (TE/TR= 20/5,000 ms). To quantify the spectra, the LCModel (Provencher 1993) was used. The LCModel facilitates metabolite separation based upon differing linear combinations of spectra of individual metabolites and estimates the concentration of each metabolite concentration by comparing the proton concentration of water in identical voxels. The GABA concentration in the basal ganglia (Fig. 2) was

Table 1 Clinical, enzymatic, and molecular characteristics of gamma aminobutyric acid transaminase (GABA-T)-deficient patients

Sign/symptom	Patient 1	Patient 2 (sib of patient 1)	This report
Intractable seizures	+	+	+
Psychomotor retardation	+	+	+
Hypotonia	+	+	+
High-pitched cry	+	+	–
Hyperreflexia	+	+	+
Lethargy	+	+	+
Acceleration of height growth	+	+	+
Age of death	25 months	12 months	Alive at 28 months
EEG/MRI/CT abnormalities	+	+	+
GABA-T (liver)[a]	70 (310–690)	–	–
GABA-T (white cells)[b]	1.2 (20–58)	–	2 (23–64)
Genotype [c]	c.[659G>A (+) 1433T>C][d]	–	c.[275G>A]+[199–?_316+?][e]
Deduced effect	p.[Arg220Lys (+) Leu478Pro]	–	p.[Arg92Gln]+[?]

EEG electroencephalograph, *MRI* magnetic resonance imaging, *CT* computed tomography, + present; – absent or not determined.

[a] Protein pmol/h/mg (control range in parentheses). [b] Protein pmol/min/mg (control range in parentheses). [c] Reference sequence NM_000663.3; missense mutations are considered to be pathogenic, as they were not encountered in 210 control chromosomes and involve highly conserved amino acids among GABA-T species. [d] Following the original publication (Jaeken et al 1984), we identified the second mutation (c.1433T>C) in the first described patient, confirming GABA-T deficiency at the DNA level. [e] In our patient, a presumed homozygous mutation was detected by direct sequence analysis; however, this was in contrast to the findings in DNA of the mother. The heterozygous mutation could not be detected in DNA of the father, therefore, a specific multiplex probe amplification test was developed. This showed the presence of a heterozygous exon deletion in DNA of the patient confirming compound heterozygosity

significantly elevated (2.9 mmol/l; normal 1.1 mmol/l±0.3, n=9), but in the semioval center, GABA elevation was slight (0.8 mmol/l; normal 0.5 mmol/l±0.2, n=9). Glutamine/glutamate complex (Glx) concentration was also slightly elevated in the semioval center (11.3 mmol/l in the basal ganglia, 8.3 mmol/l in the semioval center; normal 10.1 mmol/l ±1.5, 6.6 mmol/l±1.0, n=9, respectively). Follow-up ^{1}H-MRS analysis (at 9 months of age) revealed a more pronounced GABA elevation both in the basal ganglia and in the semioval center (5.9 mmol/l and 2.9 mmol/l, respectively). Based on these data and the results of quantitative ^{1}H-MRS, we suspected GABA-T deficiency, which was confirmed by enzyme and molecular studies in cultured lymphoblasts (Schor et al 2001) (Table 1).

Discussion

This report is on the third patient (second family) with GABA-T deficiency and the first patient in whom ^{1}H-MRS was performed. All three patients showed severe, nonspecific neurological manifestations, including psychomotor retardation, epilepsy, hypotonia, and hyperreflexia (Table 1), but our patient appeared less severely affected than the reported patients. All three also showed growth acceleration associated with increased serum growth hormone levels.

The underlying pathophysiology in GABA-T deficiency remains to be elucidated, and there is no animal model available. Evidence from animal studies indicates a neurotoxic role for supraphysiological GABA levels. For example, inhibition of GABA-T by the irreversible inhibitor, vigabatrin, induces intramyelinic edema in dogs via GABA elevation (Peyster et al 1995). Both GABA-T and SSADH deficiencies manifest seizures, which is paradoxical, as activation of the GABAergic system is predicted to be anticonvulsive. Nonetheless, it is important to remember that GABA is excitatory in the developing rodent brain and remains so for the first 1–2 weeks of life. Along these lines, the switch of GABA from a depolarizing to a hyperpolarizing response is critically important in the rodent substantia nigra pars reticulata (SNR), which has one of the highest concentrations of GABAergic neurons in the CNS (Iadarola and Gale 1982). In the murine model of SSADH deficiency, Jansen and coworkers (2008) demonstrated a significant increase in GABA in E10 embryos, which may predispose these animals to a hyperexcitatory state during development. This result, along with GABA(A) and GABA (B) receptor anomalies detected in developing SSADH-deficient mice, may reduce the seizure threshold in SSADH deficiency (Buzzi et al 2006; Wu et al 2006). Both disorders occupy juxtaposed positions in GABA degradation, and accordingly we speculate that the pathophysiological mechanisms observed in SSADH deficiency may be likely to be caused by high GABA levels, as observed in GABA-T deficiency. Neuropathology of the two index cases revealed spongy leukodystrophy, which may correspond to the white matter lesions seen on DWI in our patient. This observation may reflect changes in water motion in the axonal direction and/or axonal swelling associated with cortical neuronal damage.

Whereas ^{1}H-MRS estimates in vivo neurotransmitter concentrations (Provencher 1993), quantifying GABA in nonpathological states is difficult due to interference by much larger peaks of the glutamine–glutamate complex, creatine, and large peaks of N-acetylaspartic acid (Novotny et al. 2003). However, utilizing the LCModel facilitates separation of even low-concentration species (such as GABA) from other major compounds. Screening of the metabolite concentration by ^{1}H-MRS may readily reveal the pathological state, however, as in our patient. Moreover, the addition of a short exposure to ^{1}H-MRS may be acceptable, even in infants and children. Increased intracranial GABA detected by ^{1}H-MRS has been reported in SSADH deficiency (Ethofer et al 2004), but additional GABA-T-deficient patients require identification in order to determine how the concentrations of intracranial GABA compare to those in the same regions of SSADH-deficient patients.

In summary, GABA transaminase deficiency represents a human model of endogenous GABA elevation, which likely occurs during critical periods of human CNS development. This disorder may offer valuable insights into the role of the GABAergic system in human brain development. Our studies further suggest that quantitative ^{1}H-MRS may be clinically applicable to the inborn errors of GABA metabolism.

Acknowledgements We thank Lyuba Bayukanskaya, Ana Pop, and Rizkat Yilmaz for technical assistance. This work was supported in part by Grants-in-Aid from Scientific Research from the Ministry of Health, Labor and Welfare of Japan, Health and Labor Science Research Grant of Japan (Kokoro-Ippan-015), Takeda Science Foundation and Kanagawa Municipal Hospital Pediatric Research.

References

Buzzi A, Wu Y, Frantseva MV et al (2006) Succinic semialdehyde dehydrogenase deficiency: GABAB receptor-mediated function. Brain Res 1090:15–22

Ethofer T, Seeger U, Klose U et al (2004) Proton MR spectroscopy in succinic semialdehyde dehydrogenase deficiency. Neurology 62:1016–1018

Frahm J, Merboldt KD, Hänicke W (1987) Localized proton spectroscopy using stimulated echoes. J Magn Reson 72:502–508

Govindaraju V, Young K, Maudsley AA (2000) Proton NMR chemical shifts and coupling constants for brain metabolites. NMR Biomed 13:129–153

Iadarola MJ, Gale K (1982) Substantia nigra: site of anticonvulsant activity mediated by gamma-aminobutyric acid. Science 218:1237–1240

Jaeken J, Casaer P, de Cock P et al (1984) Gamma-aminobutyric acid-transaminase deficiency: a newly recognized inborn error of neurotransmitter metabolism. Neuropediatrics 15:165–169

Jakobs C, Jaeken J, Gibson KM (1993) Inherited disorders of GABA metabolism. J Inherit Metab Dis 16:704–715

Jansen EE, Struys E, Jakobs C, Hager E, Snead OC 3rd, Gibson KM (2008) Neurotransmitter alterations in embryonic succinate semialdehyde dehydrogenase (SSADH) deficiency suggest a heightened excitatory state during development. BMC Dev Biol 8:112

Novotny EJ Jr, Fulbright RK, Pearl PL, Gibson KM, Rothman DL (2003) Magnetic resonance spectroscopy of neurotransmitters in human brain. Ann Neurol 54(Suppl 6):S25–S31

Pearl P, Jakobs C, Gibson K (2007) Disorders of β- and γ-amino acids in free and peptide-linked forms. In The metabolic and molecular bases of inherited disease Part 8, amino acids, Ch 91. McGraw-Hill, New York

Peyster RG, Sussman NM, Hershey BL et al (1995) Use of ex vivo magnetic resonance imaging to detect onset of vigabatrin-induced intramyelinic edema in canine brain. Epilepsia 36:93–100

Provencher SW (1993) Estimation of metabolite concentrations from localized in vivo proton NMR spectra. Magn Reson Med 30:672–679

Schor DS, Struys EA, Hogema BM, Gibson KM, Jakobs C (2001) Development of a stable-isotope dilution assay for gamma-aminobutyric acid (GABA) transaminase in isolated leukocytes and evidence that GABA and beta-alanine transaminases are identical. Clin Chem 47:525–531

Wu Y, Buzzi A, Frantseva M et al (2006) Status epilepticus in mice deficient for succinate semialdehyde dehydrogenase: GABAA receptor-mediated mechanisms. Ann Neurol 59:42–52

遺伝・ゲノム学

DNAメチル化の網羅的解析

Genome wide DNA methylation analysis

DNAメチル化などのエピジェネティックな遺伝子発現制御は，ヒトの発生分化，癌などの疾患，さらには長期的な生体機能調節にかかわることが明らかにされつつある．これらの研究成果を受けてさまざまな網羅的解析が試みられているが，本稿では網羅的DNAメチル化解析のための手法をおおまかに①“区別する”，②“濃縮する”，③“検出する”の3つに分けて概説する(図1)．

“区別する”

DNAメチル化を解析するためには何らかの方法で非メチル化シトシンとメチル化シトシンを“区別”する必要がある．現在普及しているバイサルファイト法は化学反応とPCR法により非メチル化シトシンだけを最終的にチミンに置換する．置換された配列を既知の配列と比較すれば，各シトシンのメチル化状態を判定できる．置換効率や増幅の偏りなどのアーチファクトに注意が必要である一方，比較的少量の検体，固定後の組織なども解析可能であるといった利点がある．他にはDNAメチル化感受性制限酵素(メチル化DNAを切断できない酵素)を利用した方法があげられる．制限酵素の認識配列が異なれば，切断部位のゲノム上の分布も異なるので，適切な酵素を選択することで，効率的なメチル化スクリーニングを行うことができる．

“濃縮する”

現在，メチル化シトシンを特異的に認識するモノクローナル抗体を商業的に入手することができる．ゲノムDNAを適当な大きさに剪断して一本鎖にした後，上述の抗メチル化シトシン抗体で免疫沈降を行えば，メチル化DNA断片が濃縮される．また，メチル化シトシン結合蛋白質を利用した濃縮法も確立されており，二本鎖のままメチル化DNAを回収できるという特徴がある．

“検出する”

上記のような手法で区別・濃縮されたDNA断片はさらに増幅や標識化処理を行い，DNAマイクロアレイや大規模配列解析を用いて網羅的に定量することができる．マイクロアレイ上には既知配列のプローブが貼り付けられているので，区別・濃縮されたDNA断片の定量と同時にゲノム上の位置を特定することができる．すなわちメチル化部位とメチル化の程度が同定できる．さまざまなプローブのアレイ(CpGアイランドアレイ，プロモーターアレイ，タイリングアレイなど)が商品化されており，解析目的に応じたアレイを選択することが重要であるが，プラットフォームによっては比較的簡単にカスタムアレイを作製することも可能である．また，Illumina社のビーズアレイプラットフォームを利用したDNAメチル化解析法(Infiniumメチル化解析)はバイサルファイト処理後のゲノムDNAを用い，約27,000カ所のヒトCpGサイトの定量的網羅的解析が可能である．さらに，近年はアレイに加え，大規模配列解析も網羅的検出法の選択肢に入ってきた．前述の免疫沈降やバイサルファイト処理を行ったゲノムDNA断片を大量に配列決定し，位置情報とその出現頻度を解析すれば，メチル化状態を定量的に評価可能である．

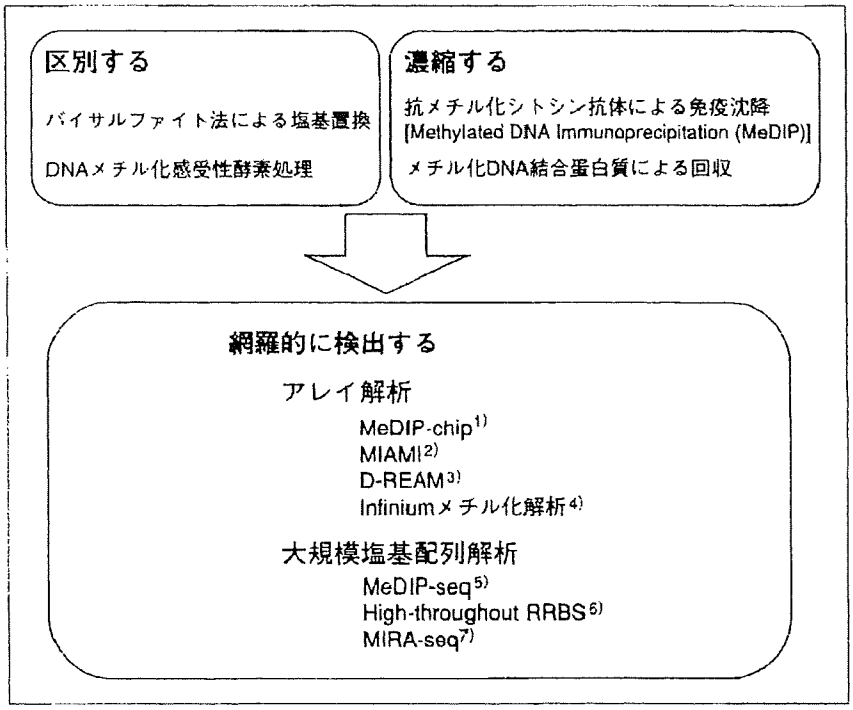

図1　網羅的DNAメチル化解析の概略

おわりに

今後このようなハイスループット技術が急速に普及するのは想像に難くないが，膨大なデータを的確に解釈するための統計学的解析ツールはまだまだ取扱いが容易とはいい難い．あるいはハイスループットとはまったく逆に，ライブ

イメージング技術や，1個の細胞といった極微量の検体を用いた網羅的 DNA メチル化解析の実現に向けて，さらなる技術的ブレークスルーが期待される．

1) Weber, M. et al.：*Nat. Genet.*, **37**：853-862, 2005.
2) Hatada, I. et al.：*Oncogene*, **25**：3059-3064, 2006.
3) Yagi, S. et al.：*Genome Res.*, **18**：1969-1978, 2008.
4) http://www.illuminakk.co.jp/product/genoTYPING/methylation_human27.shtml
5) Down, T.A. et al.：*Nat. Biotechnol.*, **26**：779-785, 2008.
6) Meissner, A. et al.：*Nature*, **454**：766-770, 2008.
7) http://genome.yonsei.ac.kr/board/lib/down.php?boarding=board_pds03 & no=49

秦健一郎／Kenichiro HATA
国立成育医療センター研究所
周産期病態研究部

Genomics 93 (2009) 461–472

Contents lists available at ScienceDirect

Genomics

journal homepage: www.elsevier.com/locate/ygeno

Identification of the mouse paternally expressed imprinted gene *Zdbf2* on chromosome 1 and its imprinted human homolog *ZDBF2* on chromosome 2

Hisato Kobayashi [a,1], Kaori Yamada [a,1], Shinnosuke Morita [a], Hitoshi Hiura [a], Atsushi Fukuda [a], Masayo Kagami [b], Tsutomu Ogata [b], Kenichiro Hata [c], Yusuke Sotomaru [d], Tomohiro Kono [a,*]

[a] Department of BioScience, Tokyo University of Agriculture, 1-1-1 Sakuragaoka, Setagaya-ku, Tokyo 156-8502, Japan
[b] Department of Endocrinology and Metabolism, National Research Institute for Child Health and Development, 2-10-1 Okura, Setagaya-ku, Tokyo 157-8535, Japan
[c] Department of Maternal-Fetal Biology, National Research Institute for Child Health and Development, 2-10-1 Okura, Setagaya-ku, Tokyo 157-8535, Japan
[d] Natural Science Center for Basic Research and Development, Hiroshima University, 1-2-3 Kasumi, Minami-ku, Hiroshima 734-8551, Japan

ARTICLE INFO

Article history:
Received 4 December 2008
Accepted 30 December 2008
Available online 4 February 2009

Keywords:
Genomic imprinting
Imprinted gene
Zdbf2
Differentially methylated region
Mouse chromosome 1
Human chromosome 2

ABSTRACT

In mammals, both the maternal and paternal genomes are necessary for normal embryogenesis due to parent-specific epigenetic modification of the genome during gametogenesis, which leads to non-equivalent expression of imprinted genes from the maternal and paternal alleles. In this study, we identified a paternally expressed imprinted gene, *Zdbf2*, by microarray-based screening using parthenogenetic and normal embryos. Expression analyses showed that *Zdbf2* was paternally expressed in various embryonic and adult tissues, except for the placenta and adult testis, which showed biallelic expression of the gene. We also identified a differentially methylated region (DMR) at 10 kb upstream of exon 1 of the *Zdbf2* gene and this differential methylation was derived from the germline. Furthermore, we also identified that the human homolog (*ZDBF2*) of the mouse *Zdbf2* gene showed paternal allele-specific expression in human lymphocytes but not in the human placenta. Thus, our findings defined mouse chromosome 1 and human chromosome 2 as the loci for imprinted genes.

Introduction

Genomic imprinting is an epigenetic gene-marking phenomenon in mammals, which leads to parent-of-origin-dependent monoallelic expression of certain genes, termed imprinted genes [1]. To date, approximately 80 imprinted genes have been identified in mice, the majority of which are present in 11 clusters including the Prader–Willi syndrome/Angelman syndrome and Beckwith–Wiedemann syndrome clusters. These clusters were assigned to 8 autosomal chromosomes, 2, 6, 7, 9, 11, 12, 15, and 17; whereas many solo imprinted genes have been identified on 5 chromosomes (numbers 2, 10, 14, 18, and 19). Many of these imprinted genes with expression patterns were well-conserved between mice and humans. These genes play an important role in fetal growth, development of particular somatic lineages, maternal behavior, tumorigenesis, and birth defects (MRC Mammalian Genetics Unit, Harwell, UK, http://www.mgu.har.mrc.ac.uk/research/imprinting/function.html).

Gene imprinting is initiated by epigenetic modifications such as DNA methylation that occur in the parental germline. In mammals, DNA methylation occurs exclusively at the cytosine residues within cytosine–guanine (CpG) dinucleotides, which plays an important role in normal development [2]. Indeed, many imprinted genes have differentially methylated regions (DMRs), which exhibit parent-of-origin-dependent DNA methylation patterns. Some DMRs function as cis-acting imprinting control regions (ICRs) that exert a regional control on gene expression from an imprinted cluster. Knockout mice studies demonstrated that the de novo DNA methyltransferase Dnmt3a and its related protein Dnmt3L are required to establish the methylation imprints in both maternal and paternal germlines [3–5]. The maintenance methyltransferase Dnmt1 is then required to maintain the differential methylation and imprinted expression patterns in the embryo proper [6,7].

A number of studies have suggested that imprinted genes may have characteristic structural features. For example, it was reported that imprinted genes tend to have fewer and smaller introns [8]. Other reports have described that human and mouse imprinted gene regions contain a lower density of short interspersed transposable elements (SINEs) than non-imprinted regions [9,10]. Thus far, the presence of direct repeats near or within the DMRs has been identified as the potential feature of these regions [11]. However, these features are not observed with regard to all imprinted regions, and their functional relevance is controversial. In a previous study, the dimensions of 15 DMRs (12 maternally imprinted genes and 3 paternally imprinted genes) were measured, and it was revealed that paternally methylated DMRs contain fewer CpGs than maternally methylated DMRs [12]. Furthermore, a recent study has demonstrated that the Dnmt3a/Dnmt3L complex could preferentially methylate CpG site pairs that are 8–10 base pairs apart, and a similar periodicity was observed for the frequency of CpG sites in the 12 maternally imprinted regions [13].

* Corresponding author. Fax: +81 354772543.
E-mail address: tomohiro@nodai.ac.jp (T. Kono).
[1] These authors contributed equally to this work.

0888-7543/$ – see front matter © 2009 Elsevier Inc. All rights reserved.
doi:10.1016/j.ygeno.2008.12.012

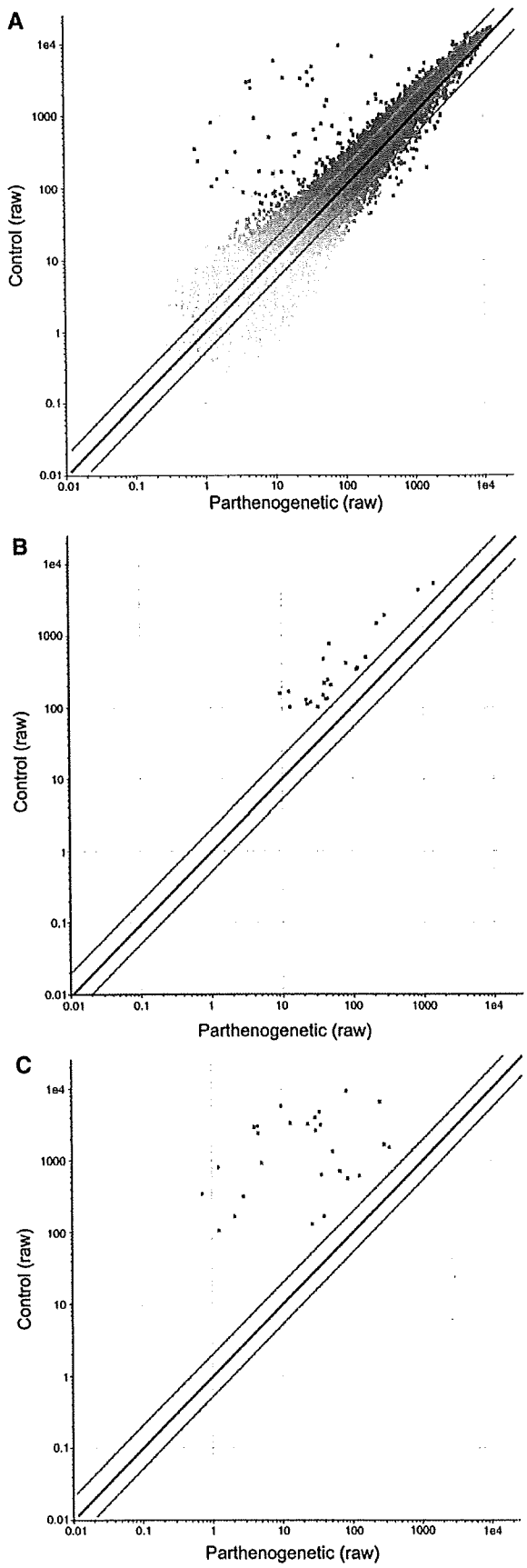

However, no other consensus sequence has been identified for DMRs, and the features that cause them to get preferentially methylated via the Dnmt3a/Dnmt3L complex in the germline remain unknown.

After the first imprinted gene, *Igf2*, was identified in a knockout study, many other methods have subsequently been used to identify imprinted genes in mice. In 1994, *U2afbp-rs* (*Zrsr1*) [14] and *Rasgrf1* [15] were identified as paternally expressed genes with the use of methylation-sensitive restriction enzyme sites as the restriction landmark in the restriction landmark genomic scanning (RLGS) method for screening methylated sites. Subsequently, Ishino's group identified 2 paternally expressed genes, namely, *Peg1* (*Mest*) and *Peg3*, and 2 maternally expressed genes, *Meg1* (*Grb10*) and *Meg3*, by comparison analysis of gene expression among in vitro fertilized parthenogenetic (containing only maternally derived chromosomes) and androgenetic (containing only paternally derived chromosomes) embryos, by suppression subtractive hybridization [16–19]. In 1997, the paternally expressed gene *Impact* was identified using allelic message display without positional cloning or production of parthenogenetic and androgenetic embryos [20]. Furthermore, the development of DNA microarray technology facilitated the identification of many imprinted genes by gene expression profiling. In 2000, Affymetrix GeneChip was used with in vitro fertilized and parthenogenetic embryos and, in 2002, RIKEN cDNA Microarray was used with parthenogenetic and androgenetic embryos to identify new imprinted genes [21,22]. Further, in 2006, Affymetrix GeneChip was used with uniparental disomies [23]. Recently, the imprinted *Mcts2* gene was identified using the sequence features of imprinted genes [24], indicating that bioinformatics analysis can contribute to the identification of novel imprinted genes. Although a recent study has estimated that there are 600 imprinted genes in mice [25], a complete global analysis for locating imprinted genes has not been performed. To elucidate the biological importance of genomic imprinting and other characteristics of imprinted genes, it is important to systematically identify the remaining imprinted genes.

In this study, we compared the gene expression profiles between parthenogenetic and in vitro fertilized embryos (control) by using the Affymetrix GeneChip probe array to identify novel imprinted genes. The control embryos containing both the maternal and paternal genomes exhibited normal expression patterns of both maternally and paternally expressed genes; however, the parthenogenetic embryos that contain 2 maternal genomes exhibited a significantly decreased expression of paternally expressed genes. On the basis of this information, we screened the imprinted gene candidates and confirmed the imprinted expression of these genes by using reverse transcriptase-polymerase chain reaction (RT-PCR) analysis. From this screening, we identified a paternally expressed imprinted gene, *Zdbf2*, on mouse chromosome 1. We also identified a DMR in the paternal allele methylated at 10 kb upstream of the predicted exon 1 of the *Zdbf2* gene. Furthermore, we demonstrated that the human homolog *ZDBF2*, which is mapped to chromosome 2, is also paternally expressed. The newly identified imprinted genes provide an opportunity to further investigate the function and mechanisms of the genomic imprinting machinery.

Results

Screening for new imprinted gene candidates by microarray analyses

In this study, we compared the global expression profiles of mouse parthenogenetic and in vitro fertilized (control) embryos by using the

Fig. 1. Comparison between the control and parthenogenetic samples. The red lines indicate equal expression levels between the 2 samples. The pink lines indicate a 2-fold change in the expression levels between the 2 samples. (A) Scatter plots of all the genes. (B) Scatter plots of candidate genes. (C) Scatter plots of known imprinted genes obtained by our screening. Partheno: parthenogenetic embryos ($n=4$); control: in vitro fertilized control embryos ($n=4$).

Table 1
Genes identified by microarray analysis between the control and parthenogenetic embryos

Control	Systematic	GenBank accession	Common name	Fold change	Control		Parthenogenetic		Chromosome
					Raw	Normalized	Raw	Normalized	
<500 raw	1423294_at	AW555393	***Mest***	96	9196.1	1	84.2	0.01	6
	1448152_at	NM_010514	***Igf2***	28.4	6508.5	1.01	253.6	0.04	7
	1426208_x_at	AF147785	***Plagl1***	97.3	5727.5	0.97	9.8	0.01	10
	1421144_at	NM_023879	*Rpgrip1*	5.5	5316.2	0.97	1460.6	0.18	14
	1433924_at	BM200248	***Peg3***	84.9	4702.7	1.02	34.5	0.01	7
	1425966_x_at	D50527	*Ubc*	5.5	4289.8	0.96	884.1	0.17	5
	1417355_at	AB003040	***Peg3***	88.2	3949.5	1.02	30	0.01	7
	1423506_a_at	AV218841	***Nnat***	97.7	3321.8	0.98	13.4	0.01	2
	1435383_x_at	AW743020	***Ndn***	90.5	3216.6	1.03	23.6	0.01	7
	1435382_at	AW743020	***Ndn***	78.7	3115.9	1.03	36	0.01	7
	1455792_x_at	AV124445	***Ndn***	99.6	2982	1	4.5	0.01	7
	1415923_at	NM_010882	***Ndn***	100.2	2871.3	1	4	0.01	7
	1437853_x_at	BB074430	***Ndn***	81.9	2585.1	1	30.3	0.01	7
	1417356_at	AB003040	***Peg3***	102.9	2394.6	1.03	4.6	0.01	7
	1417184_s_at	BC027434	*Hbb-b1*	7	1944	1.01	286.3	0.14	7
	1449939_s_at	NM_010052	***Dlk1***	6.5	1668.7	1.07	291.2	0.17	12
	AFFX-18SRNAMur/X00686_5_at	AFFX-18SRNAMur/X00686_5	*Pigt*[a]	8.9	1622	2.33	56.9	0.26	2
	1417714_x_at	NM_008218	*Hba-a1*	7.6	1470.9	1.15	222.8	0.15	11
	1415896_x_at	NM_013670	***Snrpn***	28	1336	1.01	53.4	0.04	7
	1435716_x_at	AI836293	***Snrpn***	102.7	916.7	1.04	5.1	0.01	7
	1421063_s_at	NM_033174	***Snrpn***	104.8	807.3	1.05	1.2	0.01	7
	1451058_at	AV017653	***Mcts2***	17.6	766.6	1.04	46.9	0.06	2
	1428111_at	AK003626	***Slc38a4***	16.9	710.8	1.01	67.8	0.06	15
	1448889_at	NM_027052	***Slc38a4***	31.6	629.1	1	36.6	0.03	15
	1415911_at	NM_008378	***Impact***	5.2	618.1	0.94	127.6	0.18	18
	1420688_a_at	NM_011360	***Sgce***	8.3	558.6	1.04	86.6	0.13	6
	1457356_at	BI793602	***Airn***	33.4	550	1	20.5	0.03	17
	1457781_at	BG063584	***Kcnq1***	33.4	537.2	0.97	19	0.03	7
	1455966_s_at	BG070110		5.5	502.8	1.01	156.6	0.18	[b]
	1458161_at	BM248551	***Kcnq1***	68.1	500.6	1	8.3	0.01	7
<400 raw	1456783_at	BB075402	*9330107J05Rik*	14.9	467.5	0.98	39.2	0.07	1
	1427797_s_at	BF580235		5.4	413.9	0.87	80.4	0.16	[b]
	1437213_at	BG070110		6	411.3	0.98	128.7	0.16	[b]
<300 raw	1452705_at	AK004611	*Pdxdc1*	5.5	355.2	0.59	117.4	0.11	16
	1455087_at	AV328498	***D7Ertd715e***	103	341.8	1.03	0.7	0.01	7
	1445966_at	BG075586	***Airn***	15	310.6	0.99	22.7	0.07	17
	1456139_at	BM124989	***Airn***	90.1	309.2	0.97	2.8	0.01	17
<200 raw	1451634_at	BC009123	***Airn***	19.8	271.1	1.01	19.8	0.05	17
	1427127_x_at	M12573	*Hspa1b*	5.1	240.5	0.98	45.3	0.19	17
	1436964_at	BB314814	***D7Ertd715e***	62.9	234.3	0.63	0.8	0.01	7
	1452646_at	AK003956	*Trp53inp2*	7.6	216	0.95	40.4	0.13	2
	1451386_at	BC027279	*Blvrb*	6.9	204.3	0.97	49.4	0.14	7
<100 raw	1458179_at	BB526903	***Airn***	36.6	169	1.01	6.1	0.03	17
	1424010_at	BC022666	*Mfap4*	16.3	167.1	1.04	12.6	0.06	11
	1450533_a_at	NM_009538	***Plagl1***	81.4	166.3	0.99	2.1	0.01	10
	1443007_at	AW545941	***Gnas***	8.9	162	0.94	19	0.11	2
	1439483_at	BI438039	*AI506816*	12	155.7	0.53	9.4	0.04	[b]
	1418632_at	BI694835	*Ube2h*	5.6	147.7	1.01	38.5	0.18	6
	1420978_at	NM_010938	*Nrf1*	5.1	132.4	0.9	44.6	0.17	6
	1442029_at	BM250850	***Kcnq1***	68	132.2	0.96	1.5	0.01	7
	1426009_a_at	BC003763	*Pip5k1b*	6.3	130.1	0.98	42.1	0.15	3
	1417217_at	NM_013779	***Magel2***	6.3	129.5	0.98	27	0.16	7
	1453164_a_at	AI596401	*Ptdss2*	9.8	126.2	0.99	22.1	0.1	7
	1453224_at	AW049828	*Zfand5*	8	117.9	0.99	25.8	0.12	19
	1450383_at	AF425607	*Ldlr*	5.7	110.3	0.84	23	0.15	9
	1420406_at	NM_013788	***Peg12***	71.3	105.4	0.97	1.3	0.01	7
	1434952_at	BI734783		5.7	101.8	0.95	32.2	0.17	8
	1429115_at	AK008077	*2010003O02Rik*	9.3	101.7	0.96	13	0.1	4

Genes indicated in bold are known imprinted genes.
[a] Was used as a control gene; therefore, it was excluded from the list of candidate genes.
[b] These sequences matched at more than 2 loci.

Affymetrix GeneChip assay to identify novel imprinted genes. Logically, the expression of an imprinted gene transcribed from the paternally inherited allele will be repressed in parthenogenetic embryos as compared to control embryos. In the microarray analysis, 4 parthenogenetic samples and 4 control samples were hybridized to the GeneChip (Fig. 1A). We used 2 approaches for screening candidates of paternally expressed genes. First, we excluded genes whose raw expression intensities were below 100 in the control embryos, because analysis of genes with low intensities would produce unreliable results. Second, we selected genes whose normalized data in parthenogenetic embryos was more than 5-fold lower than that of control embryos (Table 1). By this screening, we obtained 21 imprinted gene candidates (Fig. 1B), which seemed to be predominantly expressed by paternal allele, excluding 18 known imprinted genes (Fig. 1C). Of the 18 known imprinted genes obtained, 16 genes were known as paternally expressed genes. Therefore, the results of the microarray analysis were reasonable because there is down-regulation of the imprinted genes in parthenogenesis.

Identification of novel imprinted transcripts by RT-PCR

We investigated the polymorphisms in the candidate genes among C57BL/6, DBA/2, and JF1 mice in order to confirm that these candidates are true imprinted genes by allele-specific RT-PCR sequencing analysis. The polymorphism analyses of the candidate genes revealed polymorphisms in a total of 13 candidates: 2 candidates (GenBank accession numbers D50527 and NM_010938) between C57BL/6 and DBA/2 mice, 9 candidates (BB075402, AK004611, BC027279, BI694835, BC003763, AI596401, AF425607, BI734783, and AK008077) between C57BL/6 and JF1 mice, and 2 candidates (NM_008218 and BC027434) among C57BL/6, DBA/2, and JF1 mice (Table 2). To identify the alleles of these genes that were predominantly expressed, we performed RT-PCR sequencing of the candidate genes using BDF1 (C57BL6×DBA/2), DBF1 (DBA/2×C57BL/6), JBF1 (JF1×C57BL/6), and BJF1 (C57BL/6×JF1) mouse embryos at the 9.5-day-old stage (E9.5). All the primer sets for this analysis are listed in Supplemental Table 1. Allele-specific RT-PCR sequencing analysis showed that the BB075402 transcript was expressed only from the paternal allele (Fig. 2).

Expression analysis of mouse Zdbf2—a novel imprinted gene

According to the NCBI Entrez Gene database (http://www.ncbi.nlm.nih.gov/sites/entrez?db=gene), the 655-bp region of the BB075402 sequence corresponded to the 3′-untranslated region (UTR) of the *Zdbf2* (zinc finger, DNA binding factor type containing 2) gene, which contains 7 predicted exons (Fig. 3A). The *Zdbf2* gene was mapped to mouse chromosome 1C2 (Gene ID: 73884). First, we designed 3 specific primer sets (Z1, Z2, and Z3; Z1 primers were used in allele-specific RT-PCR sequencing analysis) for the 3 expressed sequence tags (ESTs) (BB075402, AK033878, and AK015271) that matched the predicted complete *Zdbf2* gene structure in order to confirm the expression levels of the gene (Fig. 3A). Incidentally, the AK033878 transcript (3113 bp) corresponds to the 3′-UTR region of the *Zdbf2* gene, and is registered as a candidate mouse imprinted transcript in the RIKEN database (http://fantom2.gsc.riken.jp/EICODB/imprinting/). The AK015271 transcript (984 bp) spliced fragment contains exons 1–7 of the *Zdbf2* gene. The microarray assay showed that the BB075402 transcript expression level in the parthenogenetic embryos was 8% (the expression level of the control was 100%) (Fig. 3B). The results of real-time PCR showed that the expression levels of the BB075402 transcript (Z1) and AK033878 (Z2) in the parthenogenetic embryos were 2% and 3%, respectively (Fig. 3C, D). Furthermore, results of the RT-PCR conducted for the AK015271 transcript (Z3) containing exons 5–7 showed a PCR band in the control embryo, but no such band was detected in the parthenogenetic embryo (Fig. 3E). Thus, we confirmed the repression of the *Zdbf2* gene in parthenogenesis. Second, we designed another primer set (Z4) for the translated region at exon 7 of the *Zdbf2* gene to confirm whether this gene is imprinted. We identified a single nucleotide polymorphism (SNP) in the Z4 region between B6 and JF1 mice. Further, allele-specific RT-PCR sequencing analysis using BJF1 and JBF1 embryos at E9.5 showed that the transcript at the Z4 region was paternally expressed (Fig. 3F). In addition, 5′-rapid amplification of cDNA ends (RACE) analysis of the *Zdbf2* gene, which was performed using BJF1 mouse embryos at E9.5, showed that the expressed transcript almost completely matched exons 1–7 of AK015271; however, exons 1 and 2 were partially matched, and exon 5 was 30 bp longer than that in the transcripts (Supplemental Fig. 1). These results suggest that the mouse *Zdbf2* gene transcript containing at least 7 exons was paternally expressed.

Expression analysis of mouse Zdbf2 in differential developmental stages and tissues

Next, we investigated the *Zdbf2* gene expression pattern in mice during 4 differential developmental stages: 15.5- and 18.5-day-old embryos (E15.5 and E18.5) and 1- and 9-week-old mice. Further, the pattern was investigated by RT-PCR analysis (at Z1 and Z4 regions) of various mouse tissues: the brain, tongue, heart, liver, lung, kidney, and muscle at all ages; the intestine and placenta in only embryos; the spleen in only 1- and 9-week-old mice; and the testis in only 9-week-old adult mice (Fig. 4). Results of the BB075402 (Z1) transcript analysis showed that gene expression was detected in almost all the major tissues from E15.5 and E18.5, except the liver and intestine, which did not show detectable expression in a few cases (Fig. 4A, Supplemental Fig. 1). Furthermore, allele-specific RT-PCR sequencing of BB075402 was performed for all the tissues (strong expression was detected) of BJF1 embryos at E15.5 and 9-week-old adult mice. Interestingly, although almost all the tissues were paternally expressed, placentas from the E15.5 embryos and adult testis exhibited biallelic expression (Fig. 4C,

Table 2
DNA polymorphism information of each paternally expressed candidate gene

Control	Gene	Nucleotide number	C57BL/6	DBA/2	JF1
< 500 raw	NM_023878	[a]			
	D50527	308	CCCTG	CCTTG	
	BC027434	232, 235	AAGAAAGT	AAAAAGGT	AAAAAGGT
	NM_008218	271	CGGTG	CGCTG	CGCTG
	BG070110	[a]			
	BB075402	589	TGAAA		TGGAA
< 400 raw	BF580235	[a]			
< 300 raw	AK004611	772	ACGTA		ACATA
	M12573	[a]			
< 200 raw	AK003956	[a]			
	BC027279	263	CCGTC		CCATC
< 100 raw	BC022666	[a]			
	BI438039	[b]			
	BI694835	154	TAAGA		TADGA
	NM_010938	1995	GAATG	GAGTG	
	BC003763	1894	GGACC		GGGCC
	AI596401	152	ATAGG		ATTGG
	AW049828	[b]			
	AF425607	395	CGATG		CGCTG
	BI734783	227	CCCAA		CCDAA
	AK008077	733	CATAG		CAAAG

All polymorphisms are shown in red.
[a] No polymorphisms were identified.
[b] No PCR bands were detected by RT-PCR.

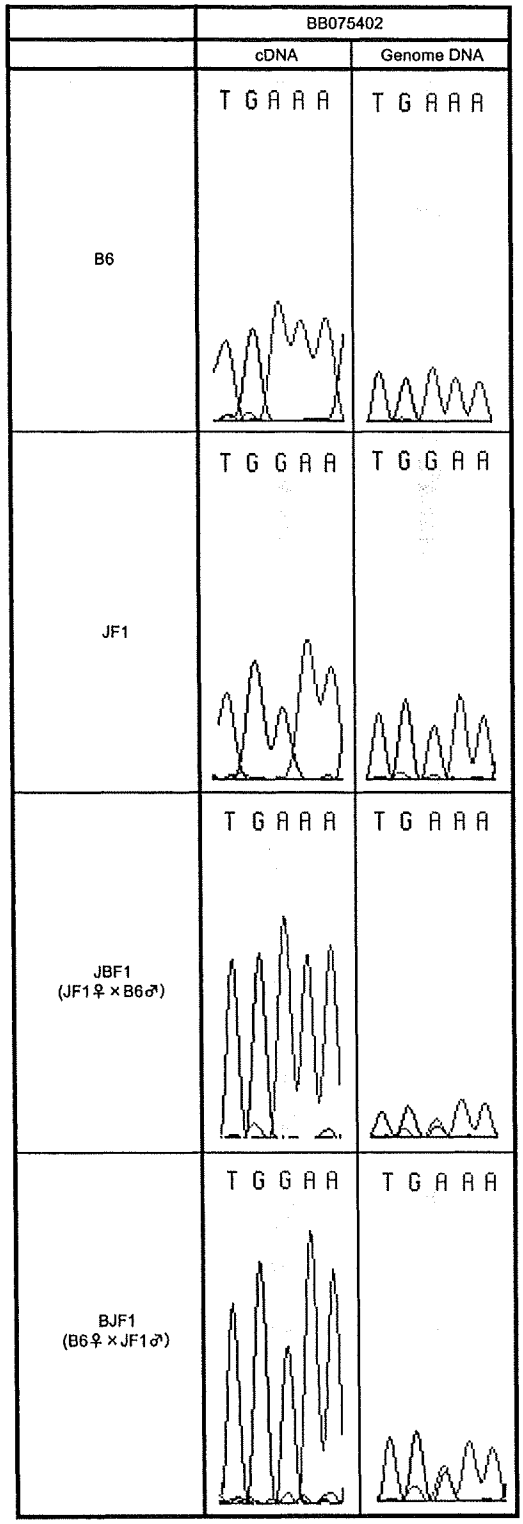

Fig. 2. Expression analysis of BB075402. Allele-specific RT-PCR sequencing analysis of BB075402 was performed with C57BL/6 (B6), JF1, BJF1, and JBF1 mouse embryos at E9.5 ($n=3$). The SNP of BB075402 is highlighted in yellow.

Supplemental Fig. 2). Meanwhile, expression at the Z4 region was detected in the brain, tongue, heart, lung, intestine, kidney, muscle, and placenta in E15.5 embryos and in the brain, tongue, kidney, muscle, and placenta in E18.5 embryos (Fig. 4B). Allele-specific RT-PCR sequencing of the Z4 region showed similar results to that of BB075402 (data not shown). These results strongly suggested that the transcript of the mouse *Zdbf2* gene is paternally expressed in almost all expressed tissues, but is biallelically expressed in only the placenta and testis.

Parent-of-origin-specific methylation of the mouse Zdbf2 gene

Many imprinted genes are epigenetically regulated by epigenetic mechanisms such as DNA methylation. DNA methylation occurs exclusively at cytosine residues within CpG dinucleotides. DMRs have been identified in CpG-rich regions (CpG islands) around imprinted genes in the maternal and paternal genomes, and it has been demonstrated that these regions function as ICRs. To explore and understand the regulation of the imprinted *Zdbf2* gene, we analyzed the DNA methylation status by using the bisulfite sequencing method [26].

The genomic DNA sequence of the mouse *Zdbf2* gene was derived from the mouse BAC clone RP23-434D24 (GenBank accession number AL669947, Fig. 5A). First, we identified 3 putative CpG islands within the AL669947 sequence using EMBOSS CpGplot (http://www.ebi.ac.uk/emboss/cpgplot/), and termed them CG1, CG2, and CG3 (Fig. 5A). These CpG islands were defined as a 200-bp stretch of DNA with a GC content of over 50% and an observed CpG/expected CpG (Obs/Exp CpG) ratio greater than 0.6. The CG1 region was observed 25 kb upstream of the *Zdbf2* gene. CG2 contains the promoter and exon 1 of the *Zdbf2* gene. We identified some SNPs in the CG1 and CG3 regions but not in CG2 by direct sequencing of samples from C57BL/6 and JF1 mice (Table 3). The CG3 contains 29 copies of the cytosine-rich 18-bp direct repeat and is included in exon 7 (Supplemental Fig. 3). To examine the differential methylation between paternal and maternal alleles in these CpG islands, we subjected them to bisulfite sequencing analyses for the CG1 and CG3 regions using 9.5-day-old in vitro fertilized embryos (BJF1 mice) and for the CG2 region using 9.5-day-old parthenogenetic and androgenetic embryos. The results showed that all the analyzed regions were almost unmethylated in both the alleles (Fig. 5B–D).

Second, by changing the CpG island criteria (minimum length, 100 bp; GC content, >50%; Obs/Exp CpG, >0.6), we identified a relatively CpG-rich region 10 kb upstream of the *Zdbf2* gene, between the CG1 and CG2 regions, and also identified SNPs in this region between C57BL/6 and JF1 mice (Table 3). We performed bisulfite sequence analysis for this region similar to the 3 CpG islands (Fig. 5E). Interestingly, paternal allele-specific methylation was detected in the CpG-rich region. Furthermore, bisulfite sequencing analyses of oocytes and sperms revealed that this region was hypomethylated in oocytes but highly methylated in sperms. These results showed that this CpG-rich region was methylated on the paternal alleles and that the methylation was derived from germline, similar to *H19* DMR, *Dlk1-Gtl2* IG-DMR, and *Rasgrf1* DMR, which are known as paternal methylation imprints [27–29]; thus, we termed this region *Zdbf2* DMR.

Human homologous ZDBF2 is paternally expressed in lymphocytes but not in the placenta

Most known imprinted genes have been identified among mammalian species, especially in mice and humans, but species-specific imprinting has been reported in some genes, like *Igf2r* and *Impact* [30,31]. To verify the imprinting status of the human homolog *ZDBF2*, we examined an SNP in the *ZDBF2* gene by direct sequencing of cDNA from human tissues. On the basis of the NCBI Entrez human gene database, the human homolog *ZDBF2* gene containing 5 exons was mapped to chromosome 2q33.3 (Gene ID: 57683), and no imprinted genes were identified on human chromosome 2. We designed a primer set within the last exon of *ZDBF2* (exon 5) including the SNP (reference SNP ID: rs10932150). We then

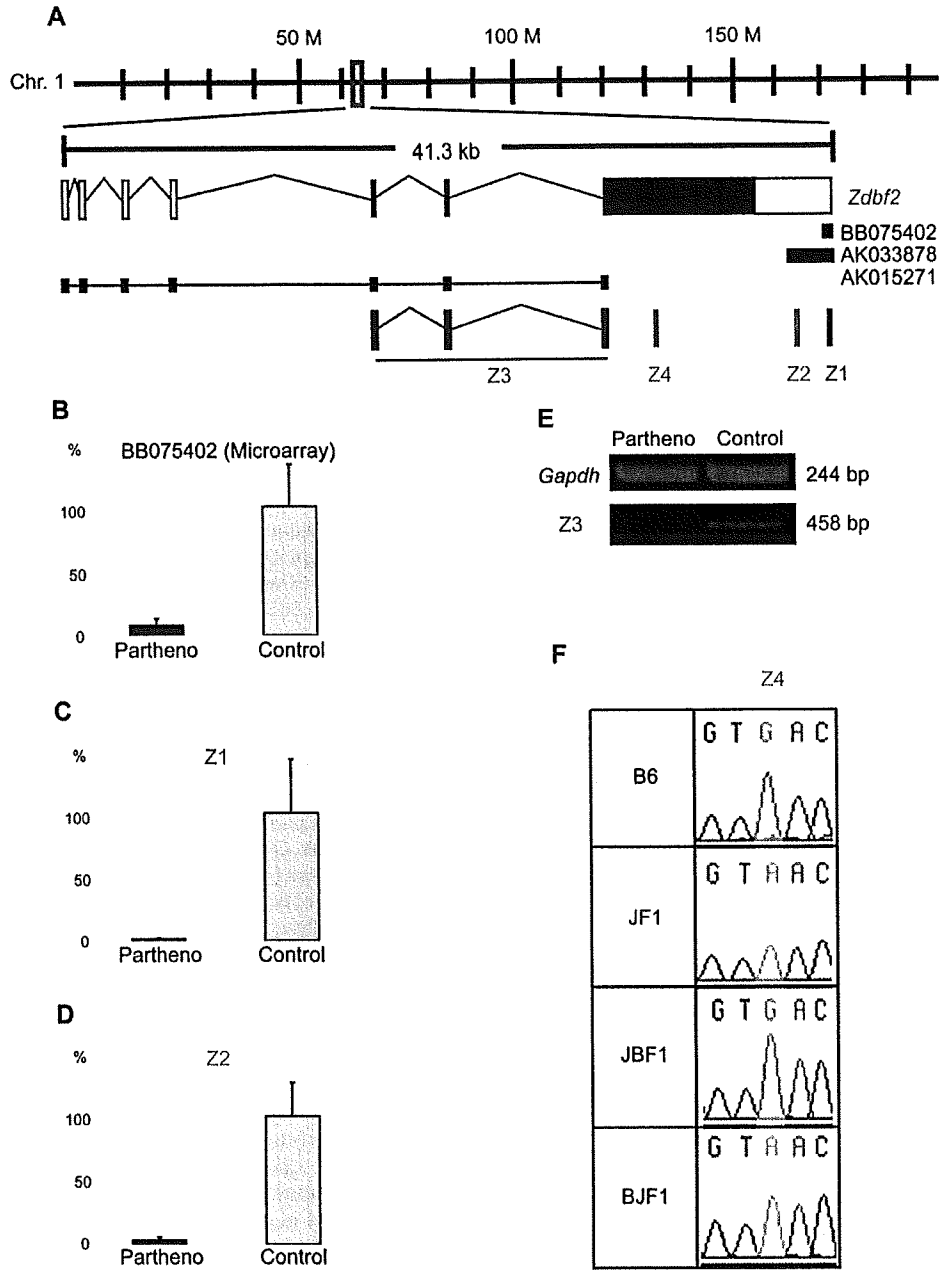

Fig. 3. Expression analysis of a novel paternally expressed gene, *Zdbf2*, on mouse chromosome 1. (A) Map of the *Zdbf2* gene on chromosome 1. Three EST positions and the primer positions of the Z1–Z4 regions are shown in the map. (B) Expression analysis of BB075402 by the microarray method. Partheno: parthenogenetic embryos ($n=4$); control: in vitro fertilized control embryos ($n=4$). Expression analysis of the Z1 (BB075402) (C) and Z2 regions (AK033878) (D) by real-time RT-PCR in the parthenogenetic ($n=3$) and control embryos ($n=3$). Values are expressed as mean ± s.e.m. (E) Expression analysis of the Z3 region (AK0152712) by RT-PCR in the control and parthenogenetic embryos. (F) Allele-specific RT-PCR sequencing analysis of the Z4 region with B6, JF1, BJF1, and JBF1 mouse embryos at E9.5 ($n=3$). The SNP of Z4 is highlighted in yellow.

performed RT-PCR analysis using human lymphocytes from a child who was heterozygous for a G/A polymorphism at the rs10932150 site, and only allele A from the father was detected (Fig. 6A, B). Furthermore, we examined the SNP in the human placenta, which was also heterozygous and, surprisingly, both G and A alleles were detected (Fig. 6C). These results revealed that the human *ZDBF2* gene is paternally expressed in lymphocytes but biallelically expressed in the placenta. This placenta-specific gene escape from imprinting is similar to that observed in the imprinted mouse *ZDBF2* gene. These results demonstrated that an imprinted locus is present on human chromosome 2.

Discussion

This study aimed to identify novel imprinted genes by comprehensive comparison of mouse gene expression. We successfully identified a imprinted gene, *Zdbf2*, which was mapped to mouse chromosome 1C2, and its imprinted human homolog, *ZDBF2*, which was mapped to human chromosome 2q33.3. The discovery of the imprinted *Zdbf2* gene may provide an opportunity to identify additional imprinted genes in the vicinity of this gene because of the clustering tendency of imprinted genes. Currently, the function of the *Zdbf2*/*ZDBF2* gene is unknown. Meanwhile, previous studies

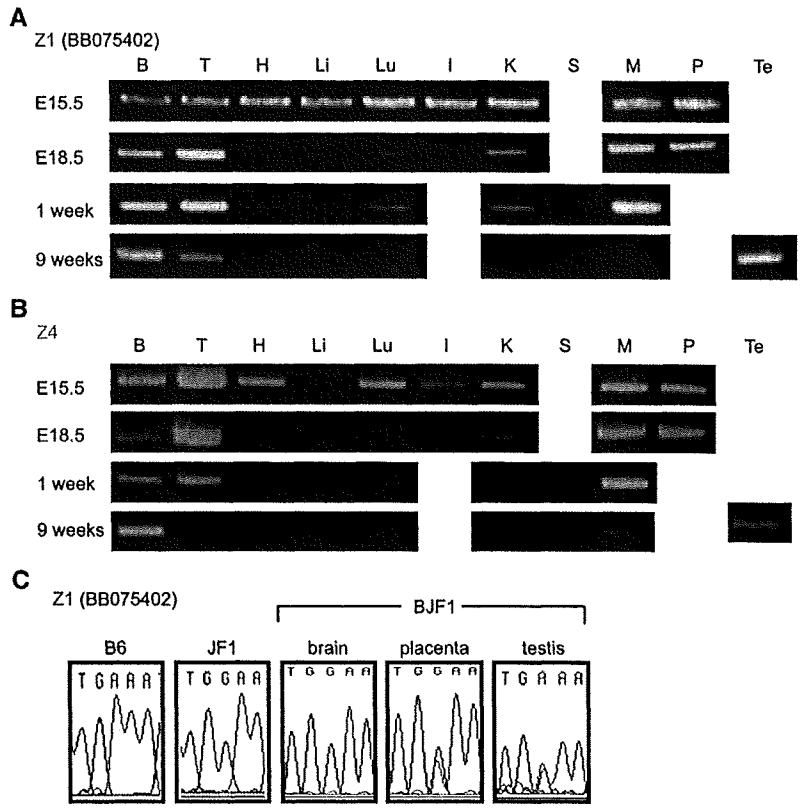

Fig. 4. Stage- and tissue-specific expression of the *Zdbf2* gene. Expression analysis by RT-PCR of Z1 (A) and Z4 (B) in the tissues (B = brain, T = tongue, H = heart, Li = liver, Lu = lung, I = intestine, K = kidney, S = spleen, M = muscle, P = placenta, and Te = testis; $n = 3$, respectively) of BJF1 mouse embryos at 15.5 and 18.5 days (E15.5 and E18.5) and 1- and 9-week-old adult mice (1 week and 9 weeks). (C) Allele-specific RT-PCR sequencing analysis of Z1 (BB075402) using B6 and JF1 mouse embryos at E9.5, the brain and placenta from BJF1 embryos at E15.5, and the testis from adult BJF1 mice ($n = 2$). The SNP of BB075402 is highlighted in yellow.

reported that maternal and paternal uniparental isodisomies for human chromosome 2 were responsible for various abnormalities [32–35]. Investigating the functions of the *Zdbf2* gene and other imprinted genes may provide further information about the imprinting disorders and mechanism.

In this study, we compared gene expression profiles between parthenogenetic and in vitro fertilized embryos (control) using the Affymetrix GeneChip probe array. We obtained 18 known imprinted genes and 21 candidates of paternally expressed genes. Some of the known imprinted genes included paternally expressed genes that were previously identified using subtraction hybridization in 9- to 10-day-old parthenogenetic and control embryos, similar to those used in our study [16,17,21,36], or embryonic fibroblast cell lines [37]. Of the obtained known imprinted genes, *Kcnq1* and *Gnas* are known as maternally expressed genes. These genes were accompanied by a paternally expressed antisense gene (*Kcnq1ot1*) or an alternative gene form (*Gnasxl*); therefore, these transcripts might be hybridized to the array [38,39]. Although we obtained several known imprinted genes from this screening, we could not obtain all the known imprinted genes. The reasons may include the decreased detection capability of tissue-specific imprinted gene expression because of RNA isolation from whole embryos or immature organ formation of each sample.

Of the 21 paternally expressed gene candidates, we identified polymorphisms among C57BL/6, DBA/2, and JF1 mice with 13 candidates. We used RT-PCR analysis and identified that of these, the BB075402 transcript was expressed only from the paternal allele. Meanwhile, many paternally expressed gene candidates exhibited biallelic expression in RT-PCR analysis. The differential expression of such genes between parthenogenetic and control embryos could be explained using 2 reasons. First, since 9.5-day-old parthenogenetic embryos exhibited delayed development as compared to the controls at the same stage of development, stage-specific genes might have been selected in this screening. Second, disruption of the imprinted gene expression in parthenogenesis might affect the expression of the non-imprinted genes, which were detected as false imprinted genes. These arguments were described in the discussion section of the previous studies [22,40]. The remaining candidate genes in which no polymorphisms were detected need to be further evaluated to determine whether they are true imprinted genes. Further investigation with other reciprocal crosses would be useful for identifying polymorphisms between the strains.

The BB075402 transcript was registered as a RIKEN mouse EST obtained from adult male diencephalons, and our study demonstrated expression of the BB075402 transcript (Z1 region) in the brain. Though almost all the major tissues showed clear expression of this transcript during embryogenesis, the tissues expressing this gene were limited to the brain, tongue, and muscle, and the testis after birth. The 3′-region of the AK033878 transcript corresponds to the BB075402 transcript, and both transcripts showed decreased expression in parthenogenetic embryos. Moreover, a part of the AK015271 transcript (Z3 region), which contains exons 1–7 of the mouse *Zdbf2* gene, was observed to show decreased expression in parthenogenetic embryos as determined by RT-PCR. We could further perform allelic expression analysis on the translated region (Z4 region shown in Fig. 3) of the mouse *Zdbf2* gene, and the results revealed that the

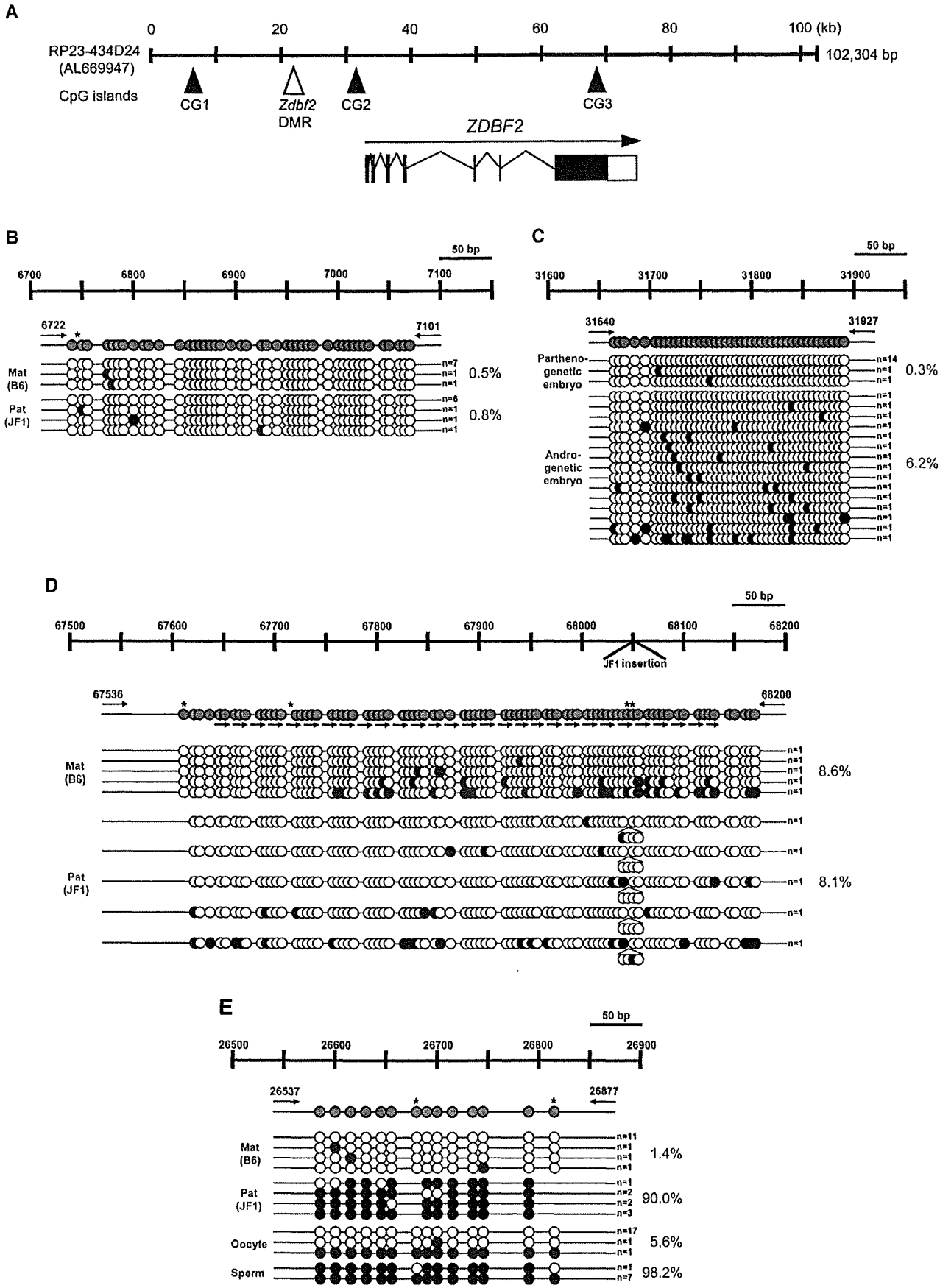
A
0
20
40
60
80
100 (kb)
RP23-434D24
(AL669947)
102,304 bp
CpG islands
CG1
Zdbf2
DMR
CG2
CG3
ZDBF2
B
50 bp
6700
6800
6900
7000
7100
6722
7101
Mat
(B6)
Pat
(JF1)
0.5%
0.8%
C
50 bp
31600
31700
31800
31900
31640
31927
Partheno-
genetic
embryo
0.3%
Andro-
genetic
embryo
6.2%
D
50 bp
67500
67600
67700
67800
67900
68000
68100
68200
JF1 insertion
67536
68200
Mat
(B6)
8.6%
Pat
(JF1)
8.1%
E
50 bp
26500
26600
26700
26800
26900
26537
26877
Mat
(B6)
1.4%
Pat
(JF1)
90.0%
Oocyte
5.6%
Sperm
98.2%

Table 3
DNA polymorphism information on each CpG-rich region surrounding the mouse *Zdbf2* gene

Region	Nucleotide number (AL669947)	C57BL/6	JF1
CG1	6753	GGAAG	GGGAG
Zdbf2 DMR	26681	CTCGA	CTTGA
	26819	TCCGA	TCTGA
CG2	a		
CG3	67619	GCGCT	GCCCT
	67716	GCCCC	GCACC
	68030	CGCGC	CGGGC
	68053	CC----------CG	CCCGTGCCCCCCGCGCGCCCCG

All polymorphisms are shown in red.
[a] No polymorphisms were identified.

translated region was paternally expressed similar to the BB075402 transcript. These results strongly indicated that these transcripts were the same products expressed solely from the paternal allele. It appeared that exons 5–6 of *Zdbf2* are also paternally expressed; however, it remained unknown as to whether the large (13 kb) transcript of the *Zdbf2* gene is expressed. Therefore, we tested 5′-RACE using mouse embryos at E15.5, and we could confirm that the expressed splice form (exons 1–7) was almost identical to the AK015271 transcript. Meanwhile, Z1 and Z4 primers did not detect expression in all the same tissues. For example, in embryonic liver, expression of the Z1 region was detectable but the Z4 region was not. Though this may be caused by the presence of different forms of the *Zdbf2* transcript in different tissues, to reveal (tissue-specific) splice variants of *Zdbf2* gene is required in future.

According to the database, the mouse *Zdbf2* gene encodes a 2493-amino acid protein with a predicted mass of 270 kDa. In our study, we demonstrated that the human *ZDBF2* gene was paternally expressed in lymphocytes. Furthermore, the human unidentified gene-encoded (HUGE) protein database of the Kazusa DNA Research Institute provides the expression profile of the human *ZDBF2* gene based on RT-PCR and enzyme-linked immuno-sorbent assay (ELISA) [41]. It is shown that the expression level of this gene in the brain and muscle is higher than that in other tissues such as those in the heart, lung, liver, kidney, pancreas, and spleen (http://www.kazusa.or.jp/huge/gfpage/KIAA1571/). Interestingly, our study showed that mouse *Zdbf2* gene expression was detected in only the brain, tongue, and muscle through the embryo to the adult stages. Thus, the expression profile of human *ZDBF2* was similar to that of mouse *Zdbf2*, which was investigated in our study. Furthermore, analyses of imprinted expression patterns showed that biallelic expression of mouse and human homologs was detected in placental tissues despite the paternal allele-specific expression observed in almost all other tissues (except for the testis) The possibility of placental tissues containing maternal materials was not completely excluded, however, the other imprinted gene (H19) showed normal imprinted expression pattern in both human and mouse placental tisses (data not shown). These facts indicate that the regulation mechanism of *Zdbf2*/*ZDBF2* gene expression is well conserved between mice and humans. Further comparison analyses of *Zdbf2*/*ZDBF2* gene products may provide hints for revealing those functions. For example, additional homologous *Zdbf2* anchors among chimpanzees, rats, dogs, horses, and chickens have been identified (Gene ID: 470622, 501153, 488490, 100068542, and 424100). These facts indicated that this gene plays an evolutionally conserved role among at least these organisms. There were no reports of the imprinted genes showed biallelic expression specifically in placenta and testis, like *Zdbf2* gene. By contract, some imprinted genes shows placenta-specific imprinted expression, and one of them, *Mash2*/*Ascl2* gene is essential for placental development [42]. The elucidation of the function of *Zdbf2* gene may explain the reason of the placenta- and testis-specific escape imprinting.

As previously noted, imprinted genes were regulated by parent-of-origin-specific DNA methylation in the DMR in *cis*. On analyzing the DNA methylation status at 4 CpG-rich regions around the mouse *Zdbf2* gene, we identified a paternal allele-specific methylated region, *Zdbf2* DMR, which is 10 kb upstream of the *Zdbf2* gene. Thus far, similar DMRs have been found in only 3 imprinted loci—*H19-Igf2*, *Dlk1-Gtl2*, and *Rasgrf*—and it has been demonstrated that these DMRs function as the ICRs controlling the neighboring imprinted genes. In particular, methylation of *H19* DMR and *Dlk1-Gtl2* IG-DMR acts as paternal methylation imprinting and prevents parthenogenesis [43,44]. Interestingly, 2 paternally expressed genes, *Igf2* and *Dlk1*, were included in the 18 known imprinted genes that were obtained from our microarray screening. This indicates that hypomethylation of *H19* DMR and IG-DMR inhibits paternally expressed genes on both maternal alleles in a parthenogenetic embryo, and that the methylation of *Zdbf2* DMR may also regulate the paternally expressed *Zdbf2* gene and the hitherto undiscovered neighboring imprinted genes. Moreover, the methylation of *Zdbf2* DMR might be established in gonocytes because the other 3 paternal methylation imprints are established in this stage [45–49], but the details of this remain unknown. The regulatory mechanism of the *Zdbf2* gene and the role of DNA methylation at the *Zdbf2* DMR should be clarified. The identification of novel paternally methylated DMRs was important and valuable, because only 3 cases showing such methylation patterns were reported, even though over 10 maternally methylated DMRs were reported. Further characterization of *Zdbf2* DMR is required to demonstrate the mechanisms by which the paternally methylated DMRs were methylated (targeted) by DNA methyltransferases. Although the real role of the repeat element in genomic imprinting [50,51] is still unknown, we identified a direct repeat sequence on the *Zdbf2* gene, similar to the other imprinted genes. In conclusion, we successfully defined mouse chromosome 1 and human chromosome 2 as the imprinted loci. Our findings provide a new platform for further identification of new imprinted genes and new insight into control of parental gene expression.

Materials and methods

Extraction of total RNA from parthenogenetic, androgenetic, and control embryos for microarray analysis

Parthenogenetic and androgenetic embryos were prepared as described previously [52]. Briefly, parthenogenetic embryos were constructed by stimulating unfertilized BDF1 eggs (C57BL6×DBA/2; Clea Japan, Tokyo, Japan) with strontium chloride solution, which contains cytochalasin B to prevent extrusion of the second polar body. Androgenetic embryos were produced by in vitro fertilization of enucleated oocytes from BDF1 mice. Pronuclear transfer (from male BDF1 mice) was performed to produce diploid androgenetic embryos. Control biparental embryos were produced by the in vitro fertilization of non-manipulated oocytes. These embryos were introduced into an

Fig. 5. Methylation profiles of *Zdbf2* DMR and CpG islands surrounding the mouse *Zdbf2* gene. (A) Genomic structure of the mouse *Zdbf2* gene. The filled vertical arrowheads indicate the positions of each CpG island, i.e., CG1, CG2, and CG3. The open vertical arrowhead indicates the position of the relatively CpG-rich region, i.e., *Zdbf2* DMR. The filled vertical arrowheads indicate the positions of each CpG island—CG1, CG2, and CG3. The methylation status of (B) CG1, (C) CG2, and (D) CG3 in the 9.5-day-old in vitro fertilized (BJF1 mice; $n=2$), parthenogenetic, and androgenetic embryos ($n=2$). Coordinates are from GenBank Sequence AL669947. The 29 continuous arrows (horizontal) indicate direct repeats within the CG3 region. (E) Methylation of *Zdbf2* DMR in the 9.5-day-old in vitro fertilized (BJF1 mice) embryos, oocytes, and sperm. The open and closed circles indicate methylated and unmethylated CpGs. The asterisks represent polymorphism positions between B6 and JF1 mice. The maternal and paternal alleles were distinguished by polymorphisms, if present, between C57BL6 (B6) and JF1 mice. Mat, maternal (B6) allele; Pat, paternal (JF1) allele. n: number of DNA clones.

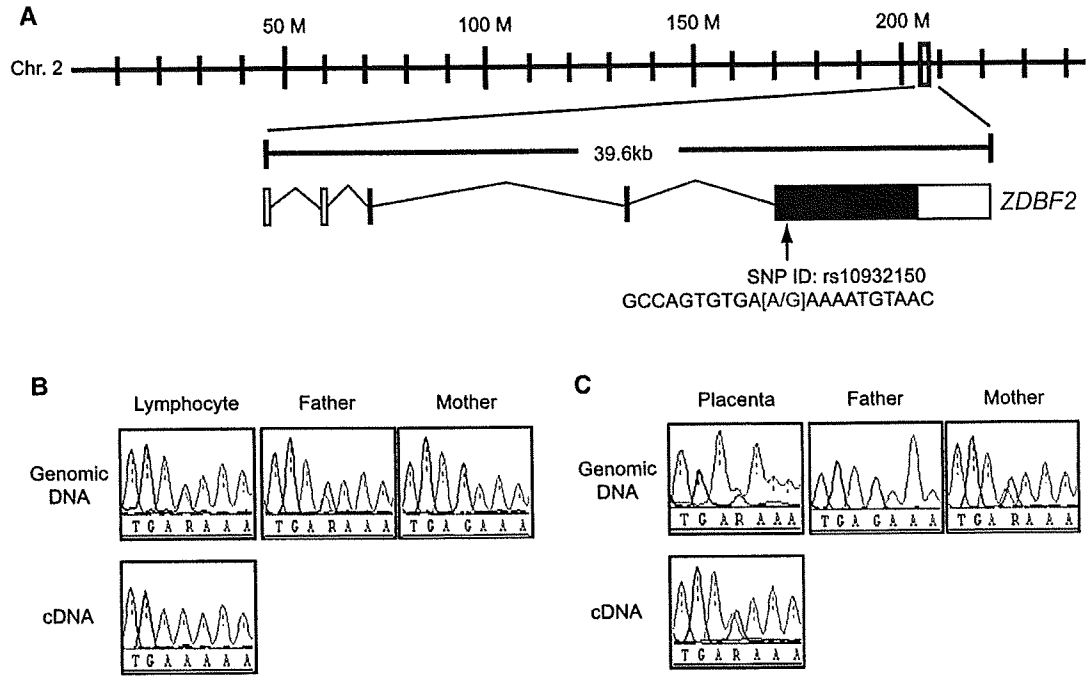

Fig. 6. Expression analysis of the *ZDBF2* gene on human chromosome 2. (A) Genomic structure of the human *ZDBF2* gene. The arrow indicates the position of the SNP (ID: rs10932150). The SNP sequence is indicated in red. Allele-specific RT-PCR sequencing analysis in (B) the human lymphocyte cell line and (C) placenta. The SNP of exon 5 is highlighted in yellow.

adult CD-1 mouse uterus. The 9.5-, 15.5-, and 18.5-day-old embryos were harvested, and TRIzol (Invitrogen, Carlsbad, CA) was used to extract total RNA from the embryos.

cRNA preparation and microarray hybridization

A 1-μg aliquot of total RNA was used as the template for cDNA synthesis (Eukaryotic Poly-A RNA Control Kit and One-Cycle cDNA Synthesis Kit; Affymetrix, Santa Clara, CA). The cDNA was purified with the Sample Cleanup Module (Affymetrix). Following cleanup, biotin-labeled cRNA was synthesized using the GeneChip IVT Labeling Kit (Affymetrix), and fragmented and purified with the Sample Cleanup Module (Affymetrix). The fragmented cRNA was hybridized with Affymetrix Mouse genome 430 2.0 GeneChip at 45 °C for 16 h. The GeneChips were then washed and stained with a GeneChip Fluidics Station 460 (Affymetrix) according to the Expression Analysis Technical Manual. An Affymetrix GeneChip Scanner 3000 was used to quantify the signal.

Microarray data analyses

The Affymetrix Mouse genome 430 2.0 GeneChip contains 45101 genes and ESTs. We compared the parthenogenetic embryos with control embryos by using the following 3 normalization methods: data transformation, where the set measurements were less than 0.01–0.01; per chip normalization, where the values were normalized to the 50th percentile to limit the range of variation; and per gene normalization, where the values were normalized to specific samples.

Polymorphism analyses among candidate genes

C57BL/6 and DBA/2 mice were purchased from Clea Japan, and JF1 mice [53] obtained from the National Institute of Genetics in Mishima, Japan. Genomic DNA was isolated from the tails of C57BL/6, DBA/2, and JF1 mice by digestion with proteinase K (Invitrogen), which was followed by phenol/chloroform extraction. The DNA was amplified by PCR with TaKaRa *Ex Taq* polymerase (TaKaRa, Kyoto, Japan). The primer sequences were complementary to the exon sequences of the candidate genes, and the PCR conditions are listed in Supplemental Table 1. The PCR products were purified with Wizard SV Gel and the PCR Clean-Up System (Promega, Madison, WI). PCR amplification was performed with TaKaRa *Ex Taq* polymerase. The purified PCR products were sequenced with primers for the direct sequence and the ABI PRISM 3130 Genetic Analyzer (Applied Biosystems, Foster, CA).

RT-PCR and allelic expression analyses among candidate genes

Using TRIzol (Invitrogen), we isolated total RNA from BDF1, DBF1 (DBA/2×C57BL/6), JBF1 (JF1×C57BL/6), and BJF1 (C57BL/6×JF1) embryos at day 9.5. After total RNA was treated with DNase (Promega) to exclude the genomic DNA, the absence of genomic DNA contamination was confirmed by the lack of amplification of GAPDH by PCR. The genomic DNA-free total RNA was reverse transcribed to cDNA with SuperScript II (Invitrogen). The expression of 22 candidate imprinted genes was examined by RT-PCR. The primer sequences and PCR conditions are listed in Supplemental Table 1 and Supplemental Table 2. To investigate the expression patterns of *Zdbf2*, different tissues at various developmental stages (15.5-, and 18.5-day-old embryos and 1- and 9-week-old mice) were harvested, and TRIzol (Invitrogen, Carlsbad, CA) was used to extract total RNA.

5′-RACE analysis

The 5′-region of the mouse *Zdbf2* gene was obtained using the 5′-Full RACE Core Set (TaKaRa). Total RNA was prepared from 9.5-day-old BJF1 embryos, and a *Zdbf2* gene-specific 5′-end phosphorylated primer (P2, 5′-ATTCCAAGGACTGCTGCTGT-3′) was used. We performed 2 rounds of PCR by using TaKaRa *LA Taq* (TaKaRa) under the following conditions: 25 cycles of 30 s at 94 °C, 30 s at 55 °C, and 4 min at 72 °C for the first PCR and 25 cycles of 30 s at 94 °C, 30 s at 60 °C, and 4 min at 72 °C for the second PCR. The primer sets

used for the nested PCR were as follows: Sense S1, 5′-TAGACCTGG-TACTTCTCAGGAACA-3′ and anti-sense A1, 5′-CAACAGATCCTGAATCC-TCGGAGT-3′ for the first PCR; sense S2, 5′-CACGCAGAAGTTGCAGTTCG-3′ and anti-sense A2, 5′-TCTGCACCGCTATCTGCAG-3′ for the second PCR. The amplified products were purified and directly sequenced.

DNA methylation analyses

Genomic DNA samples isolated from 9.5-day-old parthenogenetic, androgenetic, and control embryos or from the sperm and oocytes of adult BJF1 mice were treated with sodium bisulfite [26] using the EpiTect Bisulfite Kit (QIAGEN, Valencia, CA). The bisulfite-treated DNA was amplified by PCR with TaKaRa *Ex Taq* Hot Start Version (TaKaRa) for CpG-rich regions around the mouse *Zdbf2* gene. The primers and PCR conditions for the amplification are listed in Supplemental Table 3. The PCR products were subcloned into pGEM-T Easy vector (Promega), which was transformed into DH5α cells. Colonies were selected and transferred into 96-well plates, and DNA was amplified by rolling circle amplification [54] with an Illustra TempliPhi DNA amplification kit (GE Healthcare Bio-Sciences, Little Chalfont, UK). DNA was sequenced using standard primers (SP6, 5′-GATTTAGGTGA-CACTATAG-3′ and T7, 5′-TAATACGACTCACTATAGGG-3′) and the ABI PRISM 3130 Genetic Analyzer (Applied Biosystems). The percentage of methylation was calculated as the number of methylated CpG dinucleotides from the total number of CpGs at every CpG island (CpG-rich region). At least 5 clones from each region and each parental allele were sequenced.

Expression analysis of human ZDBF2

This study was approved by the Institutional Review Board Committee at National Center for Child Health and Development, and performed after obtaining written informed consent from each subject or his or her parent(s). Genomic DNA was isolated from human lymphocytes with the use of a FlexiGene DNA Kit (Qiagen). Total RNA was extracted from human lymphocyte cell lines with RNeasy Plus Mini Kit (Qiagen), and the total RNA from human placenta was extracted with ISOGEN (Nippon Gene, Tokyo, Japan). The extracted RNA was DNase-treated with deoxyribonuclease (RT Grade) for heat stop (Nippon Gene). DNase-treated RNA was purified by phenol/chloroform extraction. The genomic DNA-free total RNA was reverse transcribed to cDNA with SuperScript III (Invitrogen). PCR carried out in a 50-μl volume reaction mixture containing cDNA (equivalent of 20–50 ng total RNA), 1× PCR buffer, 2.5 U of AmpliTaq Gold (Applied Biosystems), 50 pmol of each primer, and 10 mM dNTPs. The primers used for human *ZDBF2* were 5′-AAACTGGA-GAAGGGACAGCA-3′ and 5′-CAAATGAGCTGCTGGTGGTA-3′. The cycling protocol was as follows: 1 min at 94 °C; 30 cycles of 94 °C for 1 min, 57 °C for 1 min, and 72 °C for 1 min; and 5 min at 72 °C.

Acknowledgments

We thank Hiroyuki Sasaki for helpful discussions. This work was supported by Grants-in-Aid for Scientific Research on Priority Area, and for Scientific Research A from the Ministry of Education, Science, Culture and Sports of Japan to T.K.

Appendix A. Supplementary data

Supplementary data associated with this article can be found, in the online version, at doi:10.1016/j.ygeno.2008.12.012.

References

[1] W. Reik, J. Walter, Genomic imprinting: parental influence on the genome, Nat. Rev. Genet. 2 (2001) 21–32.
[2] E. Li, T.H. Bestor, R. Jaenisch, Targeted mutation of the DNA methyltransferase gene results in embryonic lethality, Cell 69 (1992) 915–926.
[3] D. Bourc'his, G.L. Xu, C.S. Lin, B. Bollman, T.H. Bestor, Dnmt3L and the establishment of maternal genomic imprints, Science 294 (2001) 2536–2539.
[4] K. Hata, M. Okano, H. Lei, E. Li, Dnmt3L cooperates with the Dnmt3 family of de novo DNA methyltransferases to establish maternal imprints in mice, Development 129 (2002) 1983–1993.
[5] M. Kaneda, et al., Essential role for de novo DNA methyltransferase Dnmt3a in paternal and maternal imprinting, Nature 429 (2004) 900–903.
[6] E. Li, C. Beard, R. Jaenisch, Role for DNA methylation in genomic imprinting, Nature 366 (1993) 362–365.
[7] R. Hirasawa, et al., Maternal and zygotic Dnmt1 are necessary and sufficient for the maintenance of DNA methylation imprints during preimplantation development, Genes Dev. 22 (2008) 1607–1616.
[8] L.D. Hurst, G. McVean, T. Moore, Imprinted genes have few and small introns, Nat. Genet. 12 (1996) 234–237.
[9] J.M. Greally, Short interspersed transposable elements (SINEs) are excluded from imprinted regions in the human genome, Proc. Natl. Acad. Sci. U. S. A. 99 (2002) 327–332.
[10] X. Ke, N.S. Thomas, D.O. Robinson, A. Collins, The distinguishing sequence characteristics of mouse imprinted genes, Mamm. Genome 13 (2002) 639–645.
[11] B. Neumann, P. Kubicka, D.P. Barlow, Characteristics of imprinted genes, Nat. Genet. 9 (1995) 12–13.
[12] H. Kobayashi, et al., Bisulfite sequencing and dinucleotide content analysis of 15 imprinted mouse differentially methylated regions (DMRs): paternally methylated DMRs contain less CpGs than maternally methylated DMRs, Cytogenet. Genome Res. 113 (2006) 130–137.
[13] D. Jia, R.Z. Jurkowska, X. Zhang, A. Jeltsch, X. Cheng, Structure of Dnmt3a bound to Dnmt3L suggests a model for de novo DNA methylation, Nature 449 (2007) 248–251.
[14] Y. Hayashizaki, et al., Identification of an imprinted U2af binding protein related sequence on mouse chromosome 11 using the RLGS method, Nat. Genet. 6 (1994) 33–40.
[15] C. Plass, et al., Identification of Grf1 on mouse chromosome 9 as an imprinted gene by RLGS-M, Nat. Genet. 14 (1996) 106–109.
[16] T. Kaneko-Ishino, et al., Peg1/Mest imprinted gene on chromosome 6 identified by cDNA subtraction hybridization, Nat. Genet. 11 (1995) 52–59.
[17] Y. Kuroiwa, et al., Peg3 imprinted gene on proximal chromosome 7 encodes for a zinc finger protein, Nat. Genet. 12 (1996) 186–190.
[18] N. Miyoshi, et al., Identification of the Meg1/Grb10 imprinted gene on mouse proximal chromosome 11, a candidate for the Silver–Russell syndrome gene, Proc. Natl. Acad. Sci. U. S. A. 95 (1998) 1102–1107.
[19] N. Miyoshi, et al., Identification of an imprinted gene, Meg3/Gtl2 and its human homologue MEG3, first mapped on mouse distal chromosome 12 and human chromosome 14q, Genes Cells 5 (2000) 211–220.
[20] Y. Hagiwara, et al., Screening for imprinted genes by allelic message display: identification of a paternally expressed gene impact on mouse chromosome 18, Proc. Natl. Acad. Sci. U. S. A. 94 (1997) 9249–9254.
[21] S. Kobayashi, et al., Mouse Peg9/Dlk1 and human PEG9/DLK1 are paternally expressed imprinted genes closely located to the maternally expressed imprinted genes: mouse Meg3/Gtl2 and human MEG3, Genes Cells 5 (2000) 1029–1037.
[22] Y. Mizuno, et al., Asb4, Ata3, and Dcn are novel imprinted genes identified by high-throughput screening using RIKEN cDNA microarray, Biochem. Biophys. Res. Commun. 290 (2002) 1499–1505.
[23] R. Schulz, et al., Chromosome-wide identification of novel imprinted genes using microarrays and uniparental disomies, Nucleic. Acids Res. 34 (2006) e88.
[24] A.J. Wood, et al., A screen for retrotransposed imprinted genes reveals an association between X chromosome homology and maternal germ-line methylation, PLoS Genet. 3 (2007) e20.
[25] P.P. Luedi, A.J. Hartemink, R.L. Jirtle, Genome-wide prediction of imprinted murine genes, Genome Res. 15 (2005) 875–884.
[26] M. Frommer, et al., A genomic sequencing protocol that yields a positive display of 5-methylcytosine residues in individual DNA strands, Proc. Natl. Acad. Sci. U. S. A. 89 (1992) 1827–1831.
[27] A.C. Ferguson-Smith, H. Sasaki, B.M. Cattanach, M.A. Surani, Parental-origin-specific epigenetic modification of the mouse H19 gene, Nature 362 (1993) 751–755.
[28] H. Shibata, et al., A methylation imprint mark in the mouse imprinted gene Grf1/Cdc25Mm locus shares a common feature with the U2afbp-rs gene: an association with a short tandem repeat and a hypermethylated region, Genomics 49 (1998) 30–37.
[29] S. Takada, et al., Epigenetic analysis of the Dlk1-Gtl2 imprinted domain on mouse chromosome 12: implications for imprinting control from comparison with Igf2-H19, Hum. Mol. Genet. 11 (2002) 77–86.
[30] V.M. Kalscheuer, E.C. Mariman, M.T. Schepens, H. Rehder, H.H. Ropers, The insulin-like growth factor type-2 receptor gene is imprinted in the mouse but not in humans, Nat. Genet. 5 (1993) 74–78.
[31] K. Okamura, et al., Comparative genome analysis of the mouse imprinted gene impact and its nonimprinted human homolog IMPACT: toward the structural basis for species-specific imprinting, Genome Res. 10 (2000) 1878–1889.
[32] U. Spiekerkoetter, et al., Uniparental disomy of chromosome 2 resulting in lethal trifunctional protein deficiency due to homozygous alpha-subunit mutations, Hum. Mutat. 20 (2002) 447–451.
[33] D.A. Thompson, et al., Retinal dystrophy due to paternal isodisomy for chromosome 1 or chromosome 2, with homoallelism for mutations in RPE65 or MERTK, respectively, Am. J. Hum. Genet. 70 (2002) 224–229.
[34] B. Chavez, E. Valdez, F. Vilchis, Uniparental disomy in steroid 5alpha-reductase 2 deficiency, J. Clin. Endocrinol. Metab. 85 (2000) 3147–3150.

[35] F.M. Petit, et al., Paternal isodisomy for chromosome 2 as the cause of Crigler–Najjar type I syndrome, Eur. J. Hum. Genet. 13 (2005) 278–282.
[36] R.J. Smith, W. Dean, G. Konfortova, G. Kelsey, Identification of novel imprinted genes in a genome-wide screen for maternal methylation, Genome Res. 13 (2003) 558–569.
[37] G. Piras, et al., Zac1 (Lot1), a potential tumor suppressor gene, and the gene for epsilon-sarcoglycan are maternally imprinted genes: identification by a subtractive screen of novel uniparental fibroblast lines, Mol. Cell. Biol. 20 (2000) 3308–3315.
[38] M.P. Lee, et al., Loss of imprinting of a paternally expressed transcript, with antisense orientation to KVLQT1, occurs frequently in Beckwith–Wiedemann syndrome and is independent of insulin-like growth factor II imprinting, Proc. Natl. Acad. Sci. U. S. A. 96 (1999) 5203–5208.
[39] J. Peters, et al., A cluster of oppositely imprinted transcripts at the Gnas locus in the distal imprinting region of mouse chromosome 2, Proc. Natl. Acad. Sci. U. S. A. 96 (1999) 3830–3835.
[40] N. Ruf, et al., Expression profiling of uniparental mouse embryos is inefficient in identifying novel imprinted genes, Genomics 87 (2006) 509–519.
[41] R. Kikuno, et al., HUGE: a database for human KIAA proteins, a 2004 update integrating HUGEppi and ROUGE, Nucleic. Acids Res. 32 (2004) D502–D504.
[42] F. Guillemot, A. Nagy, A. Auerbach, J. Rossant, A.L. Joyner, Essential role of Mash-2 in extraembryonic development, Nature 371 (1994) 333–336.
[43] T. Kono, et al., Birth of parthenogenetic mice that can develop to adulthood, Nature 428 (2004) 860–864.
[44] M. Kawahara, et al., High-frequency generation of viable mice from engineered bimaternal embryos, Nat. Biotechnol. 25 (2007) 1045–1050.
[45] T.L. Davis, J.M. Trasler, S.B. Moss, G.J. Yang, M.S. Bartolomei, Acquisition of the H19 methylation imprint occurs differentially on the parental alleles during spermatogenesis, Genomics 58 (1999) 18–28.
[46] T. Ueda, et al., The paternal methylation imprint of the mouse H19 locus is acquired in the gonocyte stage during foetal testis development, Genes Cells 5 (2000) 649–659.
[47] J.Y. Li, D.J. Lees-Murdock, G.L. Xu, C.P. Walsh, Timing of establishment of paternal methylation imprints in the mouse, Genomics 84 (2004) 952–960.
[48] H. Hiura, et al., DNA methylation imprints on the IG-DMR of the Dlk1–Gtl2 domain in mouse male germline, FEBS Lett. 581 (2007) 1255–1260.
[49] Y. Kato, et al., Role of the Dnmt3 family in de novo methylation of imprinted and repetitive sequences during male germ cell development in the mouse, Hum. Mol. Genet. 16 (2007) 2272–2280.
[50] B.J. Yoon, et al., Regulation of DNA methylation of Rasgrf1, Nat. Genet. 30 (2002) 92–96.
[51] A. Lewis, K. Mitsuya, M. Constancia, W. Reik, Tandem repeat hypothesis in imprinting: deletion of a conserved direct repeat element upstream of H19 has no effect on imprinting in the Igf2-H19 region, Mol. Cell. Biol. 24 (2004) 5650–5656.
[52] Y. Obata, et al., Post-implantation development of mouse androgenetic embryos produced by in-vitro fertilization of enucleated oocytes, Hum. Reprod. 15 (2000) 874–880.
[53] T. Koide, et al., A new inbred strain JF1 established from Japanese fancy mouse carrying the classic piebald allele, Mamm. Genome 9 (1998) 15–19.
[54] J.R. Nelson, et al., TempliPhi, phi29 DNA polymerase based rolling circle amplification of templates for DNA sequencing, Biotechniques Suppl. (2002) 44–47.